Low-energy effective Hamiltonians for correlated electron systems beyond density functional theory

Motoaki Hirayama,[1] Takashi Miyake,[2] Masatoshi Imada,[3] and Silke Biermann[4]

[1]*Department of Physics, Tokyo Institute of Technology, Ookayama, Meguro-ku, Tokyo 152-8551, Japan*

[2]*Research Center for Computational Design of Advanced Functional Materials, AIST, Tsukuba 305-8568, Japan*

[3]*Department of Applied Physics, University of Tokyo, Bunkyo-ku, Tokyo 113-8656, Japan*

[4]*Centre de Physique Théorique, Ecole Polytechnique, Centre National de la Recherche Scientifique UMR7644, Université Paris-Saclay, F-91128 Palaiseau, France*

We propose a refined scheme of deriving an effective low-energy Hamiltonian for materials with strong electronic Coulomb correlations beyond density functional theory (DFT). By tracing out the electronic states away from the target degrees of freedom in a controlled way by a perturbative scheme, we construct an effective Hamiltonian for a restricted low-energy target space incorporating the effects of high-energy degrees of freedom in an effective manner. The resulting effective Hamiltonian can afterwards be solved by accurate many-body solvers. We improve this "multiscale *ab initio* scheme for correlated electrons" (MACE) primarily in two directions by elaborating and combining two frameworks developed by Hirayama *et al.* [M. Hirayama, T. Miyake, and M. Imada, Phys. Rev. B **87**, 195144 (2013)] and Casula *et al.* [M. Casula, P. Werner, L. Vaugier, F. Aryasetiawan, T. Miyake, A. J. Millis, and S. Biermann, Phys. Rev. Lett. **109**, 126408 (2012)]: (1) Double counting of electronic correlations between the DFT and the low-energy solver is avoided by using the constrained GW scheme; and (2) the frequency dependent interactions emerging from the partial trace summation are successfully separated into a nonlocal part that is treated following ideas by Hirayama *et al.* and a local part treated nonperturbatively in the spirit of Casula *et al.* and are incorporated into the renormalization of the low-energy dispersion. The scheme is favorably tested on the example of $SrVO_3$.

I. INTRODUCTION

Strongly correlated electron systems are widely found in condensed matter and have proven to generate many attractive phenomena and fundamental concepts including quantum phase transitions and fluctuations such as superconducting and metal-insulator phenomena [1] with potential applications to future technology. Their accurate and *ab initio* theoretical treatment with predictive power is therefore one of the grand challenges of contemporary condensed-matter physics. However, conventional *ab initio* computational schemes based on density functional theory (DFT) [2] or many-body perturbation theory in the so-called GW approximation (GWA) [3] are known to encounter serious difficulties when electronic correlation effects are crucial.

Recently proposed versatile multiscale method, MACE [4–6] that makes use of the hierarchical energy structure of strongly correlated electrons have opened the way to the design of increasingly accurate methods, which are now overtaking the conventional ones.

The aim of the present paper is to present a systematic scheme for the construction of improved effective Hamiltonians for low-energy degrees of freedom (L part) beyond the DFT. These effective Hamiltonians are constructed such as to contain renormalizations and screening by high-energy degrees of freedom (H part) already at the one-particle level. They present the decisive advantage that those high-energy degrees of freedom can be eliminated when solving the low-energy Hamiltonian (thus enabling the use of high-level many-body theoretical techniques) without losing their effects.

The paper is organized as follows: In Sec. II, we review some background and previous work on the construction of refined effective low-energy Hamiltonians, while in Sec. III A

we describe the general strategy to be employed. In Sec. III, we give a first outline of the equations, followed by the detailed derivations in Sec. IV. Section V presents a concise summary of the obtained scheme, while Sec. VI explains variants of the scheme. In Sec. VII, we present calculations on the perovskite oxide $SrVO_3$, illustrating how the scheme works and giving practical information on the relative importance of the different terms. The obtained effective Hamiltonian is validated by explicit dynamical mean field calculations in Sec. VIII, where it is shown that many-body calculations based on the effective Hamiltonian reproduce important features contained in higher level (GW+DMFT) calculations but not in standard DFT+DMFT, where DMFT stands for dynamical mean field theory. Finally, we present our conclusions and perspectives in Sec. IX.

II. SOME BACKGROUND ON MACE SCHEMES

In strongly correlated electron systems in condensed matter, the L part represented by the bands near the Fermi level in the DFT or GW scheme are typically sparse and isolated from the H part obtained as dense bands away from the Fermi level. This is not accidental because the isolation of the H and sparse L part is a necessary condition for strong electron correlations. (Otherwise, it would be a weakly correlated system because of the screening by the H part or by self-screening by the L part. For a more extended discussion, see [4].) MACE schemes take advantage of this hierarchical separation in the energy space to treat the L part within highly accurate but relatively expensive numerical techniques that could not be used directly for the full space in contrast to molecules and clusters treated in quantum chemistry [7–9] and nuclear physics [10,11]. For the H part,

on the other hand, cheaper techniques can be employed thanks to less significant quantum fluctuations.

Motivated by the fact that the H part behaves effectively as an insulator with a gap around the Fermi level once the dynamics within the L part is excluded, one can treat it in a controllable and accurate way by conventional methods such as the DFT within the local density approximation (LDA) or GWA. This is not in contradiction to the fact that our target materials are strongly correlated electron systems and perturbative approaches do not work as a whole, because strong correlation effects appear predominantly in the excitations within the L part that will be treated and solved afterwards beyond the LDA or GWA. Thanks to their mutual isolation, effects of the H part on the L part can be safely calculated perturbatively in the spirit of the constrained random phase approximation (cRPA) [12–14]: A partial trace summation only over the H part is taken, effectively determining the renormalization of the L part by the H part.

Physical properties of interest live in most cases on the energy scale of room temperature or below, and certainly within the L part. Therefore, an accurate treatment of the degrees of freedom in the L part is required. This low-energy system (L part) can indeed be solved using nonperturbative many-body tools, such as quantum Monte Carlo methods – in particular variational Monte Carlo [4,9,19,20], renormalization group (RG) schemes [7,8,15–18], or DMFT and related methods [5,6,21–25].

Such *ab initio* hierarchical schemes have proven useful and successful for a wide range of materials questions [4,26], from transition metals [27–31], their oxides [32–38], sulphides [39], pnictides [16,40–48], and rare earths [49–51] and their compounds [52–55], including heavy fermions [56,57], actinides [58–60] and their compounds [61] to organics [62–65], correlated semiconductors [66,67], spin-orbit materials [68–71], and correlated surfaces and interfaces [72,73]. In a hierarchical scheme such as DFT+DMFT, an effective Hamiltonian within a low-energy window around the Fermi level is obtained using DFT, and this Hamiltonian is then solved by a low-energy solver. This construction thus makes explicit use of the "separability" of high- and low-energy degrees of freedom. However, in most current schemes, little effort is devoted to the electronic structure of the higher-energy degrees of freedom—which are simply described at the DFT level—and their influence on the low-energy part.

In practice, examples where electron correlation effects were overestimated have also been found: A typical case are organic conductors [62,64], where many-body calculations using the cRPA values for the interaction—even after "dimensional downfolding" [74]—overestimate correlation effects as compared to experiments. Along the same lines, it has been argued that, in iron pnictide compounds, the ratio of the effective Coulomb interactions as estimated within the cRPA to the effective bandwidth of the Kohn-Sham band structure of the DFT is slightly overestimated as compared to experimental results [44,46,47]. On the other hand, it is known that the neglect of dynamical effects in the screening by the H part leads to an underestimation of correlation effects [75] (since the effective bandwidth is overestimated) [76]. It was proposed that this subtlety has relevance to the low-temperature metallic and nonmagnetic state of FeSe as well as the so-called

bicollinear antiferromagnetic order of FeTe [77]. A further example is the transition-metal pnictide $BaCo_2As_2$ where dynamical screening effects have been invoked to explain the puzzling absence of ferromagnetism despite a large LDA density of states at the Fermi level [78]. We will come back to these observations in the discussion section at the end of this paper.

In MACE schemes, the accurate derivation of the effective low-energy Hamiltonians or Lagrangians is crucially important for the quantitative level of the predictive power of the calculations. Therefore, the DFT or GW calculations for the global electronic structure including both the L and H part must be consistently bridged to the effective Hamiltonians in the L part. The main challenge consists in avoiding double counting of the electronic correlations and screening already taken into account at the DFT or GW level: In the DFT, Coulomb interactions are treated through the construction of an effective potential, the (Kohn-Sham) exchange-correlation potential, while the GW scheme constructs a frequency dependent many-body self-energy (albeit in a perturbative manner). On the other hand, the low-energy effective Hamiltonians or Lagrangians are solved by low-energy solvers, where the electron correlation effects are more accurately treated within this low-energy degree of freedom. Therefore, there exists overlap in treating the low-energy part of the electron correlation. This is known as the "double counting problem", and a careful and improved treatment to avoid double counting is required.

At the DFT level, the nonlinear dependence of the exchange-correlation potential on the electronic density makes the formal separation of the correlation energy contributions stemming from a subset of orbitals an ill-defined problem. On a conceptual level, strictly double-counting-free schemes are therefore only possible when avoiding the use of the DFT altogether. Double-counting-free schemes can be defined, e.g., based on many-body perturbation theory: In this case, the exchange-correlation potential is replaced by a perturbative self-energy, calculated directly in a Green's-function language. The combined "GW+DMFT" scheme [79] illustrates the advantages of such an approach. A simpler scheme, derived from the GW+DMFT, is the recently proposed "screened exchange dynamical mean field theory" [78,80,85], where the DFT exchange-correlation potential is eliminated and replaced by a screened exchange term. We also mention a recent attempt to transfer this concept to the LDA+DMFT scheme [81].

These considerations motivate the construction of effective low-energy Hamiltonians based on many-body perturbation theory for the H part, rather than on the Kohn-Sham Hamiltonian of the DFT. As we already mentioned, the perturbative treatment of the H part is indeed justified by the fact that the exclusion of excitations within the L part makes the system "insulating" with the suppressed vertex correction [4].

A disadvantage is, however, that the resulting effective models are naturally first given as Lagrangians with frequency dependent parameters in path-integral form. Indeed, integrating out the high-energy degrees of freedom generically generates frequency dependent effective interactions and hopping. It is very useful to further reduce such Lagrangians to effective Hamiltonian forms because low-energy solvers for frequency independent Hamiltonians are computationally less

demanding. In this paper, we develop a consistent and accurate *ab initio* framework of deriving the low-energy effective Hamiltonian of the L part in view of the construction of a complete MACE scheme. Our aim in the present paper is to derive low-energy effective Hamiltonians for the L space that are as accurate as possible and can be treated by sophisticated low-energy solvers in the subsequent step.

Our strategy hereby is to incorporate the effects of the frequency dependence of the effective interaction into a renormalization of the single-particle dispersion. To this end, the frequency dependent part is separated into nonlocal and local parts. The nonlocal part is treated following the perturbative scheme of Hirayama *et al.* [82] while the local part is considered nonperturbatively following Casula *et al.* [76] as detailed in Sec. III A.

III. OUTLINE OF DERIVATION OF A LOW-ENERGY EFFECTIVE HAMILTONIAN

A. General strategy

We decompose the full Hilbert space into low-energy (the L space) and high-energy subspaces (the H part) thanks to the hierarchical structure of strongly correlated electron systems as described in Sec. I. Our construction for the decomposition and bridging between the two parts will be based on the GW scheme, since this allows for a well-defined way to avoid double counting. Indeed, at the DFT level, after identifying the H and L spaces, the partial trace summation and the elimination of the H space can be performed by means of the cRPA [4,12,14], as described below. However, when the low-energy part is solved by a refined many-body solver, some parts of the interactions are counted twice since the initial DFT calculation already contains the correlation effects for the L part. Indeed, the DFT considers the exchange-correlation contribution without distinguishing the L and H spaces and it is impossible to disentangle the two spaces at this level. The GW scheme, instead, allows for the subtraction of the double counting by calculating a constrained self-energy as constructed in [82]. This constrained self-energy incorporates the interactions in the form of a self-energy from which the contribution of the L part has been excluded.

After eliminating the H space, the L space is expressed by single-, two-, and three-particle terms and even higher terms. However, the effective many-body interaction higher than the two-particle channel is expected to be small if the target L space is isolated from the H space. This is true in typical strongly correlated systems, and motivates a perturbative treatment of the H-L coupling. In this paper, we ignore multiparticle effective interactions of higher order than the two-body terms.

The single-particle (kinetic energy) terms are modified (renormalized) by the constrained self-energy. The two-particle (effective Coulomb interaction) terms are represented as the partially screened interaction obtained from the cRPA [12]. In general, the self-energy and the screened interaction are frequency dependent, thus not allowing for a representation in a Hamiltonian form.

As mentioned above, in this paper, we focus on methods that derive the low-energy effective Hamiltonians

$$H_{\text{eff}} = \sum_q T_{\text{eff}}(q) c_q^\dagger c_q + \sum_{q,k,p} W_{\text{H}}(q) c_k^\dagger c_{k+q} c_p^\dagger c_{p-q}, \quad (1)$$

where the renormalized single-particle dispersion $T_{\text{eff}}(q)$ after incorporating the self-energy effect and the effective interaction $W_{\text{H}}(q)$ screened by the H part constitute the Hamiltonian for the electrons in the L part represented by the creation (annihilation) operators for the electron, $c_k^\dagger(c_k)$ at momentum k. Here, for simplicity, spin and orbital indices are omitted.

Our task at this stage is thus to map the Lagrangians with frequency dependent single- and two-particle terms onto a frequency independent Hamiltonian in a controlled way. For this mapping, we propose a scheme that combines the merits of the works by Hirayama *et al.* [82] and Casula *et al.* [76]: In a step-by-step procedure, we include the influence of the H space into the L space and eliminate the frequency dependence by taking into account its effect on the Hamiltonian in the form of an effective renormalization of the parameters.

We remark that, in practice, the derived effective low-energy Hamiltonian satisfies the following principle: If one solved the effective low-energy Hamiltonian within the GW-type perturbative treatment instead of the accurate low-energy solver, that would yield the same result as the solution obtained by the same perturbative scheme starting from the full space including the H and L parts. This is called the "chain rule", which justifies the effective Hamiltonian as that for the L part [4,12,14].

B. Renormalized single-particle Hamiltonian

Our starting point for the single-particle part is the DFT band dispersion denoted by $\epsilon_{\text{DFT}}(q)$ and the corresponding Kohn-Sham Hamiltonian $H^{(0)} = \sum_q \epsilon_{\text{DFT}}(q) c_q^\dagger c_q$. Here, $c_q^\dagger(c_q)$ is the creation (annihilation) operator of an electron with wave vector q. We have suppressed the spin and band indices for simplicity. Then, the single-particle Green's function G_{DFT} reads

$$G_{\text{DFT}}(q,\omega) = 1/[\omega - \epsilon_{\text{DFT}}]. \quad (2)$$

On the DFT level, electronic correlations are taken into account in the form of an effective exchange-correlation potential $V_{\text{xc}}(q)$. As discussed above, treating the electron correlation effects in the L space explicitly within the low-energy solver would lead to a double counting of electronic correlation in the L space. To avoid the double counting, $V_{\text{xc}}(q)$ is subtracted and replaced by a corrective self-energy $\Delta\Sigma(q,\omega)$. By incorporating $\Delta\Sigma$, the effective single-particle part reads

$$T_{\text{eff}}(q,\omega) = \epsilon_{\text{DFT}} - V_{\text{xc}}(q) + \Delta\Sigma(q,\omega). \quad (3)$$

In the actual calculations, we propose to calculate the energies of the core electrons from DFT instead of using the GW self-energy if the computational cost is demanding. In fact, in the application to SrVO$_3$ below, we replace the DFT dispersions with the GW result only for the valence- and conduction-band parts.

C. H space contribution to self-energy: Constrained self-energy

$\Delta\Sigma$ comes from two contributions: $\Delta\Sigma = \Delta\Sigma_H + \Delta\Sigma_L$. $\Delta\Sigma_H$ is the contribution to the self-energy from the H space, while $\Delta\Sigma_L$ is from the frequency dependent part of the effective interaction incorporated into the self-energy, which is the constrained self-energy effect within the L space obtained by excluding the self-energy arising from the static effective interaction $W_H(q)$. Here, we sketch the idea for $\Delta\Sigma_H$ and discuss $\Delta\Sigma_L$ in the next subsection. A specific form for the correction $\Delta\Sigma_H$, dubbed "constrained self-energy", was already derived in [82], based on a restricted GW calculation. The basic prescription is to add only the self-energy arising from the contribution of the H space, by excluding the part stemming purely from the L space. The reason why one should exclude the self-energy stemming from the L space is that this part is more accurately calculated within the low-energy solver afterwards.

D. Renormalization to self-energy from frequency dependent partially screened interaction

The cRPA [12] was proposed as a means to calculate the effective local Coulomb interactions to be used in the L space from a systematic first-principles procedure. It can be understood as a way of tracing out the H space for deriving the effective interaction, while keeping track of the resulting renormalization of the L space degrees of freedom. The tracing out of the H space by the standard cRPA results in an effective interaction for the two-particle part in the L space in the form

$$W_H(q,\omega) = \frac{v(q)}{1 - P_H(q,\omega)v(q)}, \tag{4}$$

where the wave-number (q) dependent bare Coulomb interaction v is partially screened by the partial polarization P_H. Here, P_H is defined in terms of the total polarization P by excluding the intra-L space polarization P_L: $P_H \equiv P - P_L$. P_L involves only screening processes within the L space.

Here, W_H is frequency dependent as schematically illustrated in Fig. 1. However, most many-body calculations in the literature that use the effective interactions from the cRPA method or similar schemes neglect this frequency dependence (exceptions are [75,76,78,82–89]), and use only the zero-frequency value of the interaction $W_H(q,\omega = 0)$ for the construction of the low-energy effective Hamiltonian [12,82].

We note that this static limit $W_H(q,\omega = 0)$ obtained by using Eq. (4) in fact satisfies the above-mentioned chain rule: The whole dynamical interaction emerging when one solves the whole H and L space degrees of freedom by RPA is the usual fully screened interaction $W(q,\omega)$ given by

$$W(q,\omega) = \frac{v(q)}{1 - P(q,\omega)v(q)}, \tag{5}$$

as is depicted in Fig. 1.

On the other hand, if we calculate the screening by the RPA within the L space by regarding as if $W_H(q,\omega = 0)$ would be the bare interaction, this leads to a screened interaction

$$W_L(q,\omega) = \frac{W_H(q,\omega = 0)}{1 - P_L(q,\omega)W_H(q,\omega = 0)}, \tag{6}$$
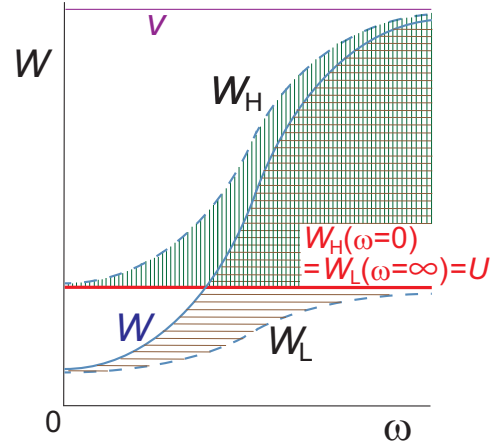

FIG. 1. Schematic frequency dependence of effective interaction screened from bare interaction v, and obtained from full RPA (GW) (W), cRPA (W_H), and screened interaction by RPA (W_L) within low-energy effective Hamiltonians at the effective interaction $U = W_H(\omega = 0)$. This is only a qualitative feature and more realistic dependence is seen in Fig. 10.

which is depicted schematically in Fig. 1. Here, P_L is the RPA polarization in the low-energy subspace. Note that $W_L(q,\omega \to \infty) = W_H(q,\omega = 0)$. Then the chain rule $W_L(q,\omega = 0) = W(q,\omega = 0)$ can be proven [12].

However, the static $W_H(q,\omega = 0)$ amounts to neglecting the frequency dependent part

$$W_H^{\text{dyn}}(q,\omega) \equiv W_H(q,\omega) - W_H(q,\omega = 0) \tag{7}$$

depicted by the vertical hatching in Fig. 1. In this paper, we will take into account the contribution of this dynamical part as the renormalization to the kinetic-energy part, either as a perturbative self-energy or in a nonperturbative fashion. In the effective low-energy Hamiltonian, we then keep $W_H(q,\omega = 0)$ for the effective interaction. In the case of the perturbative treatment, for example, the contribution to the self-energy $\Delta\Sigma_L$ is

$$\Delta\Sigma_L^{\text{Pert}} = G_L W_H^{\text{dyn}}(q,\omega) \tag{8}$$

as was formulated in [82] and which we review in detail in the next section.

We also remark that the dynamical part to be considered can be improved from Eq. (7) in a more consistent manner: Since the screening on the RPA level within the L space is W_L in Eq. (6), one realizes that the dynamical part of the interaction ignored when we use the low-energy solver is

$$W_{GW}^{\text{dyn}}(q,\omega) \equiv W(q,\omega) - W_L(q,\omega) \tag{9}$$

depicted as the horizontal hatching in Fig. 1.

Then we need to take into account the renormalization (namely, self-energy effect) originating from $W_{GW}^{\text{dyn}}(q,\omega)$ instead of $W_H^{\text{dyn}}(q,\omega)$. The perturbative contribution to the self-energy then replaces Eq. (8) with

$$\Delta\Sigma_L^{GW} = G_L W_{GW}^{\text{dyn}}(q,\omega). \tag{10}$$

Using $W_{GW}^{\text{dyn}}(q,\omega)$ in Eq. (10) replacing $W_H^{\text{dyn}}(q,\omega)$ is expected to improve the self-energy, because it takes into account the

missing part of the L space dynamics on the GW level and satisfies the chain rule even for the self-energy as we show in the following.

A conventional one-shot GW calculation in the full space gives full self-energy from the fully screened Coulomb interaction W [Eq. (5)] as

$$\Sigma = G_{\mathrm{L}} W. \quad (11)$$

(Note: We write here and in the following symbolically GW. Depending on if the calculation is done on the real/Matsubara axis, a factor -1 or i has to be added.) On the other hand, the self-energy within the L space at the one-shot GW level is

$$\Sigma_{\mathrm{L}} = G_{\mathrm{L}} W_{\mathrm{L}}. \quad (12)$$

Then $\Sigma = \Delta\Sigma_{\mathrm{L}}^{GW} + \Sigma_{\mathrm{L}}$ is obviously satisfied, which is the chain rule for the self-energy. In this paper, we compare the results calculated from the two choices Eqs. (7) and (9) in examples to gain physical insights.

Note that the interaction is not additive, but—at the GW level—the self-energy is. Our formalism is entirely based on the additivity of the self-energy. The additive expressions of the interaction in Eqs. (7) and (9) are used only to obtain the self-energy corrections. On the RPA (GW) level, the self-energy correction to be subtracted is Eq. (12), because this is the self-energy when the low-energy effective Hamiltonian is solved in the RPA level, while it will be solved within a more refined many-body solver later. On the other hand the full self-energy at the RPA level is given by Eq. (11). Equations (8) and (10) are just the results of the subtraction of Eq. (12) from Eq. (11).

We emphasize again that both Eqs. (7) and (9) are for the frequency dependent part of the partially screened interaction, which vanishes in the limit $\omega \to 0$ and is small in the energy range of the L space (see Fig. 1). The subtracted true low-energy part, either $G_{\mathrm{L}} W_{\mathrm{H}}(\omega = 0)$ or $G_{\mathrm{L}} W_{\mathrm{L}}$, will be replaced by the solution of an accurate low-energy solver. In this sense, this treatment can also be regarded as another (additional) constrained Hartree-Fock/GW scheme, employed this time for the frequency dependent part.

The effective Hamiltonian is then given by

$$H_{\mathrm{eff}} = \sum_q T_{\mathrm{eff}}(q,\omega) c_q^\dagger c_q$$
$$+ \sum_{q,k,p} W_{\mathrm{H}}(q,0) c_k^\dagger c_{k+q} c_p^\dagger c_{p-q}, \quad (13)$$

with T_{eff} given by Eq. (3) by employing either $\Delta\Sigma_{\mathrm{L}}^{\mathrm{Pert}}$ or $\Delta\Sigma_{\mathrm{L}}^{GW}$ for $\Delta\Sigma_{\mathrm{L}}$ contained in $\Delta\Sigma$ in Eq. (3). Equation (13) still contains the frequency dependence in T_{eff}, which should be incorporated in the frequency independent form by including the renormalization effect.

Then, on top of the zero-frequency limit $T_{\mathrm{eff}}(q,\omega = 0)$, to incorporate the effects of the frequency dependence, we implement the following procedure: First, the frequency dependence in the nonlocal part of W_{H} is taken into account perturbatively. This is done by constructing a self-energy $\Delta\Sigma(q,\omega)$ along the lines of [82]. This proposal employs $\Delta\Sigma_{\mathrm{L}}(q,\omega) = G_{\mathrm{L}} W^{\mathrm{dyn}}$, where W^{dyn} is either $W_{\mathrm{H}}^{\mathrm{dyn}}$ or W_{GW}^{dyn}. Thus the incorporated renormalized single-particle part is linearized in ω as $T_{\mathrm{eff}}(q,\omega = 0) - [d\Delta\Sigma(q,\omega)/d\omega]\omega$, and the ω dependence is absorbed into the renormalization factor $Z_{\mathrm{corr}} = 1/[1 - d\Delta\Sigma(q,\omega)/d\omega|_{\omega=0}]$, where the dispersion $T_{\mathrm{eff}}^{(0)}(q)$ is replaced with $Z_{\mathrm{corr}} T_{\mathrm{eff}}^{(0)}(q)$.

The effects of the local part of the interaction are taken into account following the proposal by Casula *et al.* [76]. There it was shown that—in the antiadiabatic limit—a Lagrangian with frequency dependent interactions can be mapped onto a Hamiltonian with static interactions and a renormalized one-body part. The renormalization factor Z_B can be explicitly obtained from the frequency dependence of the interaction. We will give the explicit form in the next section.

As a result, the single-particle part of the effective Hamiltonian Eq. (1) as defined by its hopping $T_{\mathrm{eff}}^{(0)}(q)$ is replaced by a single-particle Hamiltonian with effective hopping

$$T_{\mathrm{eff}}^{(1)}(q) = [\epsilon_{\mathrm{DFT}} - V_{\mathrm{xc}} + \Delta\Sigma(q,\omega = 0)]Z_{\mathrm{corr}} Z_B, \quad (14)$$

which replaces $T_{\mathrm{eff}}(q,\omega)$ in Eq. (13) and the Hamiltonian form (1) is obtained.

IV. DETAILED DERIVATION OF EFFECTIVE HAMILTONIANS

In this section, we give a detailed description of the derivation of the effective Hamiltonians outlined above.

A. Starting point

We start from the "noninteracting" Hamiltonian $H^{(0)}(k)$, and assume that we are working in a basis where its single-particle part is block diagonal at each k point (e.g., in a Wannier gauge associated with atom-centered Wannier functions constructed separately for the L and H spaces). We will think of $H^{(0)}$ as the Kohn-Sham Hamiltonian of the DFT, even though other choices are possible. We assume that the block diagonality should be a good starting point, because in many typical correlated materials such as typical transition-metal oxides the bands that have dominated the character of the localized orbitals are energetically separated from itinerant bands such as ligand bands. This fact helps the construction of effective Hamiltonians since it implicitly guarantees the existence of such a basis set. Indeed, vertex corrections that would mix the two spaces decrease with the energetic separation.

A consequence of the block diagonality is that the noninteracting Green's function $G^{(0)}$ is also block diagonal and can be decomposed into

$$G^{(0)} = G_{ll}^{(0)}|L\rangle\langle L| + G_{hh}^{(0)}|H\rangle\langle H| \quad (15)$$

where the bra-kets are a shorthand for projectors onto the respective subspaces.

We stress that Σ in Eq. (11) is not in general block diagonal. Rather, it has both off-diagonal and diagonal components, e.g.,

$$\Sigma_{lh} = G_{ll}^{(0)} W_{lllh} + G_{hh}^{(0)} W_{lhhh} - V_{xclh}, \tag{16}$$

$$\Sigma_{ll} = G_{ll}^{(0)} W_{llll} + G_{hh}^{(0)} W_{lhhl} - V_{xcll}. \tag{17}$$

Here, $G_{ab}^{(0)} = -\langle T c_a(\tau) c_b^\dagger(0) \rangle$, where a and b denote elements of the H or L spaces, and W_{abcd} is the coefficient of the interaction term $c_a^\dagger c_b c_c^\dagger c_d$. In the following, we will use the convention that l and h represent degrees of freedom belonging to L and H degrees of freedom, respectively.

This matrix is used to calculate the interacting Green's function

$$G(q,\omega) = [G^{(0)-1} - \Sigma]^{-1}. \tag{18}$$

Straightforward matrix inversion gives for the ll block (low-energy block) of this Green's function

$$G(q,\omega)_{ll} = \frac{1}{G_{ll}^{(0)-1} - \Sigma_{ll} - \Sigma_{lh} G_{hh} \Sigma_{hl}}. \tag{19}$$

In the following, we will use this form to extract a corrective self-energy: The latter is given by those parts of $\Sigma_{ll} + \Sigma_{lh} G_{hh} \Sigma_{hl}$ that are generated by the presence of the H space. This self-energy contribution should be taken into account at the level of the construction of the low-energy effective Hamiltonian, as an effective renormalization of the L space by the H space.

B. Interspace exchange term

The last term in the denominator of Eq. (19) is an "interspace exchange" self-energy contribution originating from the block-off-diagonal self-energy Σ_{lh} (Σ_{hl}) between L and H electrons. While it can in principle be treated by a direct calculation, we prefer to disregard it at this stage. The reason is that, within the low-energy subspace, it is in fact a higher-order (second-order) contribution in the interspace interaction. The interspace exchange interaction is expected to be small if the H and L spaces are well separated. In addition, the interspace exchange may at least partially cancel with the first-order vertex term.

C. Direct H space contribution to constrained self-energy

The corrective self-energy that we are interested in here is thus contained in the second to last term in the denominator of Eq. (19), the block-diagonal self-energy Σ_{ll} given by Eq. (17). This quantity includes some influence of the high-energy H space through (a) the screened Coulomb interaction W_{llll} in the first term and (b) the entire second term. Here, W_{llll} is either $W_H(q,\omega)$ in Eq. (4) or $W(q,\omega)$ in Eq. (5) and the first term contains $\Delta\Sigma_L$. This former part will be discussed in the next subsection. The latter gives

$$\Delta\Sigma_H(q,\omega) = G_{hh}^{(0)} W_{lhhl}. \tag{20}$$

As we will see below its effect is a band narrowing with respect to the Hartree band structure, comparable to the effect of the exchange-correlation potential V_{xc} of the DFT.

This correction can either be applied directly as a frequency dependent additional self-energy term $\Delta\Sigma_H(q,\omega)$, in which case it leads to a dynamical low-energy model, or one can use a Taylor expanded approximate form. If the low-energy behavior is to a good approximation linear, that is, its frequency dependence is well approximated as

$$\Delta\Sigma_H(q,\omega) = \Delta\Sigma_H(q,\omega=0) + \Delta\Sigma_H'|_{\omega=0}\omega, \tag{21}$$

where $\Delta\Sigma_H' = d\Delta\Sigma_H/d\omega$, then the renormalization factor resulting from this contribution is given by

$$Z_H = \frac{1}{1 - \frac{\partial\Delta\Sigma_H(q,\omega)}{\partial\omega}\big|_{\omega=0}}. \tag{22}$$

At this level the effective kinetic energy is renormalized to

$$T_{\text{eff}}^{(1)}(q) = [\epsilon_{\text{DFT}} - V_{xc} + \Delta\Sigma_H(q,\omega=0)]Z_H. \tag{23}$$

D. Frequency dependence of interactions within low-energy space: Nonlocal part

We finally analyze the remaining term $G_{ll}^{(0)} W_{llll}$, the first term in Eq. (17). The low-energy effective Hamiltonian or Lagrangian has to be constructed in such a way that—at the GW level within the L space—this self-energy would be reproduced. The influence of the H space, contained in this term through the matrix element of the fully screened interaction W or W_H, hereby has to enter in an effective way.

This can be naturally achieved when constructing a Lagrangian with the dynamical interaction $W_H(q,\omega)$ as given in Eq. (4). One thus obtains at first a Lagrangian with nonlocal and frequency dependent interactions, and the task is to map this Lagrangian onto a frequency independent Hamiltonian form by effectively renormalizing the Hamiltonian parameters. For that purpose, we treat the nonlocal and local parts of the interaction (two-body) terms separately. Here, we define the local part of the interaction by the Wannier function, which is written as $\Sigma_q W(q)$. We first eliminate the frequency dependence in the nonlocal part by treating it within the perturbative scheme proposed by Hirayama et al. [82]. The perturbative treatment is justified, because the corresponding correction is small. On the other hand, the local and frequency dependent part can be large and we will treat it nonperturbatively in the formalism proposed by Casula et al. [76]. This procedure allows for a nonperturbative treatment but is only suitable for local interactions. An additional subtlety arises due to the fact that the nonperturbative treatment does not take on the form of a self-energy but rather a direct renormalization of the hopping. Therefore, no zero-frequency part appears in the procedure by Casula et al., and we therefore retain the local static part explicitly as an additional correction on equal footing as the nonlocal one.

In practice, we first reduce the problem to a low-energy many-body problem where only the local interactions are dynamical, but nonlocal ones are static. Following the strategy of Hirayama et al. [82], we treat the nonlocal dynamical part of the interactions in a perturbative fashion. This amounts to (a) replacing the nonlocal dynamical interactions $[W_R^{\text{dyn}}(q,\omega)]_{\text{nonlocal}} \equiv W_R(q,\omega) - \sum_q W_R(q,\omega)$ by static nonlocal interactions $[W_R(q,\omega=0)]_{\text{nonlocal}}$ and (b) treating the frequency dependent correction $W_R^{\text{dyn}}(q,\omega)$ perturbatively as an additional self-energy correction. $W_R^{\text{dyn}}(q,\omega)$ takes on the

form defined in Eq. (7) or Eq. (9) depending on whether the Hartree-like treatment (denoted as $R = $ H) or the GW-like treatment (denoted as $R = GW$) is chosen, and—depending on this choice—leads to the correction Eq. (8) or Eq. (10), respectively.

Such a perturbative correction can be done in two different ways: The straightforward option is simple first-order perturbation theory in the difference $[W_R^{\text{dyn}}(q,\omega)]_{\text{nonlocal}}$. This part contains the effects of the frequency dependence of the interaction neglected in the effective Hamiltonian formalism with $W_R(q,\omega = 0)$. Again R denotes either the Hartree-like or GW-like treatment ("H" or "GW"). We will discuss both options in the following paragraphs.

1. Direct perturbation theory

To first order in W, the simple perturbative option results in a correction term (for simplicity, we drop the frequency summation here)

$$\Delta\Sigma_{\text{L}}^{\text{nonlocal}}(q) = \sum_{q'} G^{(1)}(q')\left[W_{\text{H}}^{\text{dyn}}(q+q')\right]_{\text{nonlocal}}$$

$$\equiv \sum_{q'} G^{(1)}(q')\left[W_{\text{H}}^{\text{dyn}}(q+q')\right.$$

$$\left. - \sum_q W_{\text{H}}^{\text{dyn}}(q+q')\right]$$

$$\simeq \left[\sum_{q'} G^{(1)}(q')W_{\text{H}}^{\text{dyn}}(q+q')\right]_{\text{nonlocal}}. \quad (24)$$

Here,

$$G^{(1)-1} \equiv G^{(0)-1} + V_{\text{xc}} - \Delta\Sigma_{\text{H}}, \quad (25)$$

and $W_{\text{H}}^{\text{dyn}}(q,\omega)$ is defined in Eq. (7). We stress that the last line of Eq. (24) is not strictly the same as the first line because of the nonzero overlap of the single- and two-particle Wannier bases, as discussed in the Appendix and in [87]. Nevertheless, as discussed in the Appendix, for sufficiently localized basis sets, the difference between the two previous lines of Eq. (24) is tiny and will be neglected hereafter. In later discussions, we describe this nonlocal part of the self-energy in a simplified notation as

$$\Delta\Sigma_{\text{L}}^{\text{nonlocal}}(q) = G^{(1)}\left[W_{\text{H}}^{\text{dyn}}(q)\right]_{\text{nonlocal}} \text{ or equivalently}$$

$$= \left[G^{(1)}W_{\text{H}}^{\text{dyn}}(q)\right]_{\text{nonlocal}}. \quad (26)$$

2. GW-type perturbation theory

Alternatively, a more refined perturbation theory inspired by the GW approximation can be constructed for the nonlocal part of Eq. (10) as

$$\Delta\Sigma_{\text{L}}^{\text{nonlocal}} = G_{ll}^{(0)}W_{GW}^{\text{dyn}} - G_{ll}^{(0)}\left[W_{GW}^{\text{dyn}}\right]_{\text{local}}. \quad (27)$$

Here, W_{GW}^{dyn} as defined in Eq. (9) corresponds to the frequency dependent part of the interaction that would be missing if the low-energy part were solved within the GW approximation. This justifies to employ the static effective interaction $W_{\text{L}}(q,\omega = 0) = W_{\text{L}}(q,\omega \to \infty)$, because $W_{\text{L}}(q,\omega)$ is the GW

counterpart of what will be treated within the low-energy solver afterwards.

We note that without the subtraction of the local part, this correction would correspond to what has been constructed as $\Delta\Sigma_{\text{L}}$ by Hirayama *et al.* in [82]. The local part is not touched here since it will be treated nonperturbatively below, following the work by Casula *et al.* [76].

Here, $G^{(0)}$ is used in the spirit of a (non-self-consistent) "one-shot GW" scheme. If one employs a (partially) self-consistent version of the GW scheme, $G^{(0)}$ may be replaced by $G^{(2)}$ defined by

$$G_{ll}^{(2)-1} \equiv G_{ll}^{(0)-1} + V_{\text{xc}} - \Delta\Sigma_{\text{H}} - G_{ll}^{(0)}W. \quad (28)$$

At this level the effective dispersion is renormalized to

$$T_{\text{eff}}^{(1)}(q) = [\epsilon_{\text{DFT}} - V_{\text{xc}} + \Delta\Sigma_{\text{H}}(q,\omega = 0)$$

$$+ \Delta\Sigma_{\text{L}}(q,\omega = 0)]Z_{\text{HL}}, \quad (29)$$

where $Z_{\text{HL}} = \{1 - d[\Delta\Sigma_{\text{H}}(q,\omega) + \Delta\Sigma_{\text{L}}^{\text{nonlocal}}(q,\omega)]/d\omega|_{\omega=0}\}^{-1}$. Note that here we have included $\Delta\Sigma_{\text{L}}^{\text{local}}(q,\omega = 0)$ as a direct correction, as discussed above. Together with the nonlocal part $\Delta\Sigma_{\text{L}}^{\text{nonlocal}}(q,\omega = 0)$ it is thus the full $\Delta\Sigma_{\text{L}}(q,\omega = 0)$ that enters.

E. Intra-*d* exchange

The resulting many-body problem with long-range interactions will have an intra-L space exchange self-energy contribution of Fock form. Also this term takes different forms depending on whether one places oneself in the perspective of the option in Sec. IV D 1 or in Sec. IV D 2 above.

1. Direct perturbation theory

In the first case, the exchange term is the simple Fock exchange calculated with the static interaction $W_{\text{H}}(q,\omega = 0)$:

$$\Delta\Sigma_{\text{L}}^x = G_{ll}^{(1)}W_{\text{H}}(q,\omega = 0). \quad (30)$$

Once this term has been taken into account, only the correlation part of the self-energy will have to be calculated within the low-energy effective Hamiltonian.

However, in most practical many-body calculations, local exchange contributions will be kept within the low-energy description in the form of Hund's coupling terms. We therefore prefer to incorporate only the nonlocal contribution in the one-shot GW as

$$\Delta\Sigma_{\text{L}}^{x\,\text{nonlocal}} = G_{ll}^{(1)}W_{\text{H}}(q,\omega = 0) - \sum_q\left[G_{ll}^{(1)}W_{\text{H}}(q,\omega = 0)\right]$$

$$(31)$$

into the effective one-body Hamiltonian while keeping the local one as a many-body term.

An interesting cancellation is observed when the intra-L space exchange is combined with the above correction $\Delta\Sigma_{\text{L}}^{\text{nonlocal}}$; the remaining correction

$$\Delta\Sigma_{\text{L}}^{\text{nonlocal}} + \Delta\Sigma_{\text{L}}^{x\,\text{nonlocal}}$$

$$= \left\{G_{ll}^{(1)}[W_{\text{H}}(q,\omega) - W_{\text{H}}(q,\omega = 0)]\right\}_{\text{nonlocal}}$$

$$+ \left[G_{ll}^{(1)}W_{\text{H}}(q,\omega = 0)\right]_{\text{nonlocal}}$$

$$= \left[G_{ll}^{(1)}W_{\text{H}}(q,\omega)\right]_{\text{nonlocal}} \quad (32)$$

reduces to the nonlocal part of a dynamical Fock term, calculated with the interaction $W_H(q,\omega)$, that is, the bare interaction within the low-energy space.

2. GW-type perturbation theory

If, however, the GW-like option is chosen for eliminating the frequency dependence of the nonlocal interactions in the low-energy subspace (Sec. IV D 2 above), the intra-L space exchange should accordingly be interpreted as a screened exchange term. In practice, this means that again a GW-type expression has to be adopted:

$$\Delta\Sigma_L^{x\ \text{nonlocal}} = \left[G_{ll}^{(0)}W_L(q,\omega)\right]_{\text{nonlocal}}. \tag{33}$$

Combining this term with the above $\Delta\Sigma_L^{\text{nonlocal}}$, a similar cancellation as above is observed:

$$\begin{aligned}
\Delta\Sigma_L^{\text{nonlocal}} &+ \Delta\Sigma_L^{x\ \text{nonlocal}} \\
&= \left\{G_{ll}^{(0)}\left[W(q,\omega) - W_L(q,\omega)\right]\right\}_{\text{nonlocal}} \\
&\quad + \left[G_{ll}^{(0)}W_L(q,\omega)\right]_{\text{nonlocal}} \\
&= \left[G_{ll}^{(0)}W(q,\omega)\right]_{\text{nonlocal}}.
\end{aligned} \tag{34}$$

The final correction is thus simply the nonlocal part of the usual GW self-energy [90].

At this stage, the effective dispersion is renormalized to

$$\begin{aligned}
T_{\text{eff}}^{(1)}(q) = [&\epsilon_{\text{DFT}} - V_{\text{xc}} + \Delta\Sigma_H(q,\omega = 0) \\
&+ \Delta\Sigma_L^{\text{nonlocal}}(q,\omega = 0) \\
&+ \Delta\Sigma_L^{x\ \text{nonlocal}}(q,\omega = 0)]Z_{\text{HW}}
\end{aligned} \tag{35}$$

where

$$\begin{aligned}
Z_{\text{HW}} = \big\{1 - d\big[&\Delta\Sigma_H(q,\omega) + \Delta\Sigma_L^{\text{nonlocal}}(q,\omega) \\
&+ \Delta\Sigma_L^{x\ \text{nonlocal}}(q,\omega)\big]/d\omega|_{\omega=0}\big\}^{-1}.
\end{aligned} \tag{36}$$

F. Frequency dependence of interactions within low-energy space: Local part

The remaining problem is one with dynamical local interactions, for which the *correlation part* of the self-energy should be calculated. It can be reduced to a problem with purely static interactions following Casula *et al.* [76]: The recipe is to replace the local dynamical interactions by static local interactions while at the same time renormalizing the one-body part of the problem. A subtlety consists, however, in defining which dynamical interactions to take. We again differentiate the two options above. We also note that the self-energy from local dynamical interaction at zero frequency $\Delta\Sigma_L^{\text{loc}}(\omega = 0)$ is already taken into account in Eq. (29).

1. Direct perturbation theory

In this case, the additional renormalization factor resulting from the frequency dependence of the local interaction is the one derived in the original work by Casula *et al.*: Indeed, $W_H^{\text{loc}}(\nu) \equiv \sum_q W_H(q,\nu)$, the effective dynamical interaction in the low-energy subspace corresponds to what is usually considered as local "Hubbard U", and its frequency dependence

determines the renormalization factor according to

$$Z_B = \exp\left(1/\pi \int_0^\infty d\nu \text{Im}W_H^{\text{loc}}(\nu)/\nu^2\right). \tag{37}$$

2. GW-type perturbation theory

The GW-type strategy yields a more involved recipe: Defining the local part of Eq. (9), namely,

$$\left[W_{GW}^{\text{dyn}}(\omega)\right]_{\text{local}} = \sum_q (W - W_L), \tag{38}$$

one can consider that the Lagrangian to be treated as this stage is one with an interaction the static part of which is given by $W_H(q,\omega = 0)$ while its dynamical part reads $[W_{GW}^{\text{dyn}}]_{\text{loc}}$. (By construction W_{GW}^{dyn} vanishes at zero frequency.) The corresponding renormalization is given by

$$Z_B = \exp\left(1/\pi \int_0^\infty d\nu \text{Im}\left[W_{GW}^{\text{dyn}}(\nu)\right]_{\text{loc}}/\nu^2\right). \tag{39}$$

V. SUMMARY OF THE SCHEME

Putting the above steps together, one obtains the total constrained self-energy

$$\Delta\Sigma = \Delta\Sigma_H + \Delta\Sigma_L^{\text{nonlocal}} + \Delta\Sigma_L^{x\text{nonlocal}} \tag{40}$$

resulting in the following scheme:

(1) Calculate the LDA Hamiltonian in the localized basis. Block diagonalize it.

(2) Calculate the sum of the correction self-energies above:

$$\Sigma_{\text{corr}}(q,\omega) = -V_{\text{xc}} + \Delta\Sigma. \tag{41}$$

If the simple perturbative strategy is adopted, we employ $\Sigma_{\text{corr}} = \Sigma_{\text{corr}}^{\text{Pert}}$ (see Secs. IV D 1 and IV E 1):

$$\Sigma_{\text{corr}}^{\text{Pert}}(q,\omega) \equiv -V_{\text{xc}} + G_{hh}^{(0)}W_{lhhl} + \left[G_{ll}^{(1)}W_H\right]_{\text{nonlocal}}. \tag{42}$$

Following the GW-type perturbation theory, it becomes $\Sigma_{\text{corr}} = \Sigma_{\text{corr}}^{GW}$ (see Secs. IV D 2 and IV E 2):

$$\Sigma_{\text{corr}}^{GW}(q,\omega) \equiv -V_{\text{xc}} + G_{hh}^{(0)}W_{lhhl} + \left[G_{ll}^{(0)}W\right]_{\text{nonlocal}}. \tag{43}$$

This self-energy can be linearized, e.g., around the Fermi level, giving rise to a static correction $\Sigma_{\text{corr}}(q,\omega = 0)$ and a Z factor corresponding to its (linearized) frequency dependence:

$$Z_{\text{corr}} = \frac{1}{1 - \frac{\partial\Sigma_{\text{corr}}(q,\omega)}{\partial\omega}\big|_{\omega=0}}. \tag{44}$$

(3) The effect of the local dynamical interaction is taken into account as follows: Calculate the renormalization factor Z_B arising from the local part of the frequency dependence in the screened interaction (see Secs. IV F 1 and IV F 2).

(4) The effective low-energy Hamiltonian is eventually given by

$$\begin{aligned}
H_{\text{eff}}^{(1)} = &\sum_q T_{\text{eff}}^{(1)}(q)c_q^\dagger c_q \\
&+ \sum_{q,k,p} W_r(q,0)c_k^\dagger c_{k+q}c_p^\dagger c_{p-q}
\end{aligned} \tag{45}$$

with

$$T_{\text{eff}}^{(1)}(q) = [\epsilon_{\text{DFT}} + \Sigma_{\text{corr}}(q,\omega = 0)]Z_{\text{corr}}Z_B. \tag{46}$$

(5) Solve the many-body problem with the one-body Hamiltonian from the preceding step and the static nonlocal interactions $W_H(q,\omega = 0)$. Take care of removing the Hartree contribution from the solution of the many-body problem, in order to avoid double counting with the initial single-particle Hamiltonian where the Hartree potential was included in LDA. This can be done by following the procedure in [82], where the Hartree solution of the low-energy effective Hamiltonian is subtracted before solving by the low-energy solver. This can also be done as in LDA+U or LDA+DMFT techniques, by calculating the Hartree solution of the effective low-energy Hamiltonian.

VI. VARIANTS OF THE LOW-ENERGY HAMILTONIAN

The above discussion has focused on the construction of an effective low-energy many-body problem with static and local interactions, for which only the correlation part of the self-energy needs to be calculated from the many-body solver. Alternatively, if one uses a many-body solver that can fully handle long-range interactions, a variant of the above scheme can be envisioned. Another variant can be used if one wishes to construct a low-energy Hamiltonian with purely local interactions only. A different variant is useful if one wishes to update the single-particle part of the Hamiltonian, after an improved estimate for the electronic density is available after the many-body calculation. This is the subject of the following paragraphs.

A. Low-energy Hamiltonian with long-range interactions

If the aim is the construction of a low-energy effective Hamiltonian with fully long-range Coulomb interactions, the treatment of the intra-L space exchange term can be omitted at the level of the construction of the Hamiltonian. The remaining corrective self-energy reads

$$\Sigma_{\text{corr}}(q,\omega) = \Delta\Sigma_H + \Delta\Sigma_L^{\text{nonlocal}}$$
$$= G_{hh}^{(0)}W_{lhhl} + G_{ll}^{(0)}W_H^{\text{dyn}} - \left[G_{ll}^{(0)}W_H^{\text{dyn}}\right]_{\text{local}} \quad (47)$$

where the option of direct perturbation theory W_H^{dyn} defined in Eq. (7) should be replaced by W_{GW}^{dyn} defined in Eq. (9) for the option of the GW-type perturbation theory.

We note, however, that the reduction to a static Hamiltonian using the Casula procedure involves in this case an additional approximation: Indeed, strictly speaking, the Casula procedure modifies the non-density-density terms of the interactions, by dressing the creation and annihilation operators with exponential weight factors. This can be seen as follows: The Casula procedure is based on a Lang-Firsov transformation [91], replacing the original fermionic operators $c_{i\sigma}$ at the ith site with spin $\sigma(=\uparrow$ or $\downarrow)$, by polaronic operators $d_{i\sigma}$, thus eliminating the explicit dependence on the bosonic operators b_i that describe the screening degrees of freedom: $d_{i\sigma} = \exp[\lambda(b_i - b_i^\dagger)]c_{i\sigma}$. While the exponentials drop out for density-density terms, since $d_{i\sigma}^\dagger d_{i\sigma} = c_{i\sigma}^\dagger c_{i\sigma}$, this is not true for more general interactions. In principle, the corresponding correction factors can be worked out by straightforward operator algebra. For simplicity, we will, however, disregard

here this complication, assuming, e.g., that any long-range interactions are of pure density-density type.

B. Effective Hamiltonian with local Hubbard interactions only

The solution of the final many-body problem with nonlocal interactions may in principle be done within many-body solvers suitable for nonlocal interactions such as various Monte Carlo methods including the variational Monte Carlo [19,20]. Alternatively, extended DMFT [92,93] can be viewed as a means to determine an effective local interaction that best represents the effects of the initial long-range interactions, and can be considered as a technique to "backfold" long-range interactions into effective local ones.

Very generally, from the above discussion it becomes obvious that the construction of the one-particle part of the Hamiltonian will depend on which interaction terms will be included in the many-body calculation, while physical properties obtained after solving the low-energy problem are expected to be insensitive to the choice. In the next section, we will see how the derived effective Hamiltonians behave in the case of the simple oxide $SrVO_3$.

C. Update of the single-particle Hamiltonian

In some cases, many-body effects substantially change the charge distribution in the low-energy subspace as compared to the LDA one. Such redistributions of charge can, for example, happen between different orbitals in multiorbital systems, and have actually been observed, e.g., in titanium oxides [94], $BaVS_3$ [39], or iron-based superconductors [43,77]. If this happens, one might want to update the starting Hamiltonian and GW self-energies, based on the new charge density rather than the converged LDA one, analogously to what is done in the DFT+DMFT calculations [52,58]. This effect can induce non-negligible corrections to the relative orbital levels.

Technically, the resulting self-consistency loop is analogous to what has been discussed in detail in the DMFT literature [95], in particular concerning the way the density is recalculated in the continuum after the solution of the effective Hamiltonian.

VII. RESULTS

The ternary $3d^1$ transition-metal oxide $SrVO_3$ has become one of the "drosophila compounds" of correlated systems. It is a correlated metal that has been characterized using various experimental [96–102] and theoretical techniques (see, e.g., [41,87–89,94,95,103–110]). A review of most of the available experimental and theoretical data has been given recently in [89]. $SrVO_3$ displays Fermi-liquid behavior up to remarkably high temperatures of the order of 200 K [97,102], with a moderate mass enhancement of the order of 2 [101,111]. Detailed spectroscopic investigations have made it an ideal test compound for modern many-body calculations, and more and more refined dynamical mean field based studies are available. The majority of studies so far have focused on the t_{2g} manifold which forms the states close to the Fermi level, and those will also be the focus in the present investigations. Note, however, that this restriction quite severely limits the range of validity of the low-energy description. Indeed, as shown recently [88,89]
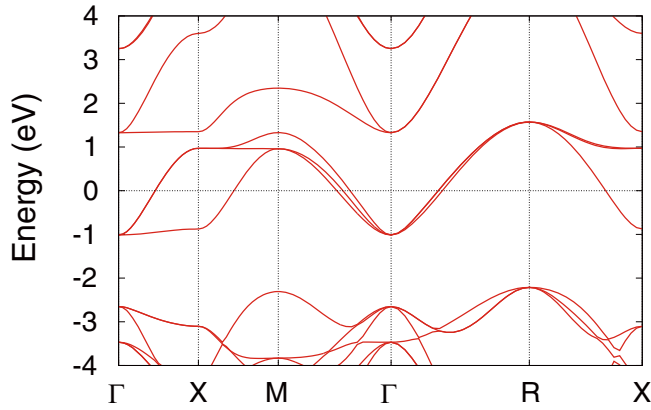
FIG. 2. Kohn-Sham band structure of $SrVO_3$ in the LDA. The energy is measured from the Fermi level.

at energies of about 2 to 3 eV above the Fermi level the spectral properties are largely determined by the e_g states. This has in particular led to a reinterpretation of an inverse photoemission feature at about 2.5 eV that was frequently interpreted as an upper Hubbard band of t_{2g} character in the earlier literature. Here, we use the compound only as an illustration of the principles of constructing effective low-energy Hamiltonians, without being concerned with a description of spectra beyond the pure t_{2g} part.

The LDA band structure of $SrVO_3$ is shown in Fig. 2. One clearly distinguishes the threefold degenerate manifold of t_{2g} bands close to the Fermi level (chosen as the zero of energy), followed in the unoccupied part of the spectrum by the two e_g bands. At about -2.5 eV the filled O-$2p$ derived bands are visible.

When a standard GW calculation is performed, see Fig. 3, the bandwidth of the t_{2g} states is reduced from 2.5 to 2.1 eV, while the overall shape of the dispersion remains similar to the LDA one. This is in agreement with previous GW calculations in the literature [87–89,110].

The calculation is based on the full-potential linear muffin-tin orbitals implementation. An $8 \times 8 \times 8$ mesh is
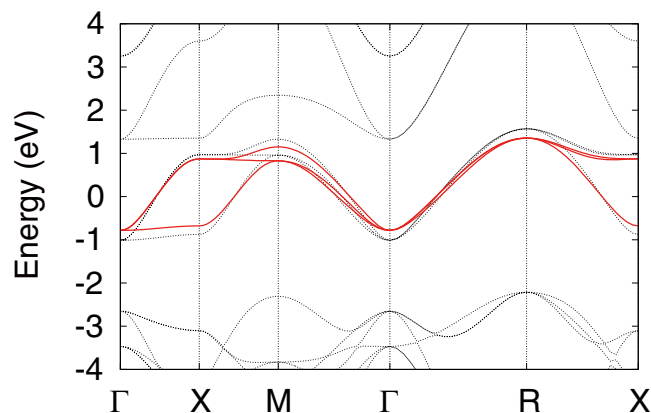
FIG. 3. Band structure of $SrVO_3$ in the one-shot GW approximation. For comparison, the LDA band structure is also given (black dotted line). The energy is measured from the Fermi level.
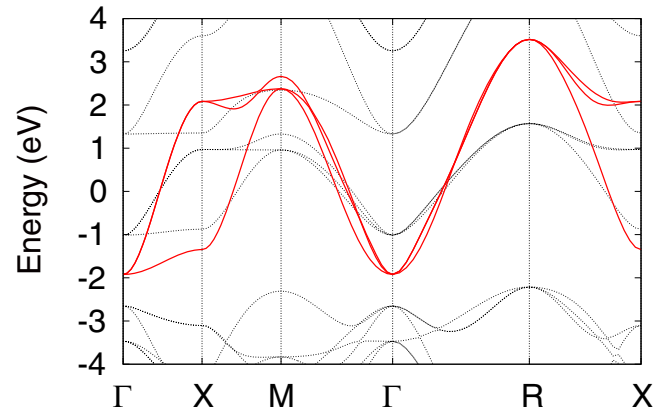
FIG. 4. Band structure of $SrVO_3$ corresponding to the LDA Hamiltonian from which the LDA exchange-correlation potential has been subtracted. For comparison, the LDA band structure is also given (black dotted line). The energy is measured from the Fermi level.

employed in both the DFT/LDA and the GW calculations. The calculational details are the same as in [82].

We now turn to a discussion of the band structure corresponding to the Hamiltonians to be used as input for subsequent many-body calculations for this material. We will proceed step by step to analyze the influence of the various correction terms, with respect to the DFT starting point (which will be overlaid to the respective band structures).

Figure 4 displays the band structure corresponding to the LDA Hamiltonian from which the LDA exchange-correlation potential has been subtracted, that is, the eigenvalues of $H_{LDA} - V_{xc}$ where these operators are evaluated for the self-consistent LDA density. The subtraction of V_{xc} widens the band structure from the LDA bandwidth of 2.5 eV to more than twice this value: the new bandwidth is 5.4 eV. This indicates that the exchange-correlation potential V_{xc} of the LDA is responsible for a substantial amount of the band-narrowing effect arising from electronic correlations, stressing the need to subtract the double counting in a consistent manner. Figure 4 is regarded as the starting point for the following considerations.

For simple materials (see, e.g., the calculations on Li in [112]) it has been noted in the literature that the Hartree band structure is close to the DFT one. This raises the question of the origin of the substantial band widening in the present case. Indeed, the present calculation shown in Fig. 4 differs from a Hartree calculation only by the fact that Fig. 4 is evaluated for the converged LDA density. We have performed a test calculation where we plot the Hartree band structure calculated for the converged Hartree density. The result is shown in Fig. 5. As seen from this plot, while the band is not fully as wide as in Fig. 4, a substantial widening is already present at this stage.

Starting from the Hamiltonian without V_{xc} (see the dispersion in Fig. 4), we first take into account the static part of the corrective self-energy $\Delta\Sigma_H$: In Fig. 6, we plot the dispersion corresponding to $H_{LDA} - V_{xc} + \Delta\Sigma_H(\omega = 0)$. Compared to the dispersion of Fig. 4, the overall band structure is narrowed to 3.7 eV. This value is, however, still considerably larger than the LDA bandwidth (Fig. 2). Although the electronic correlations coupling the H and the L space are included in Fig. 6, and narrow the band with respect to the case
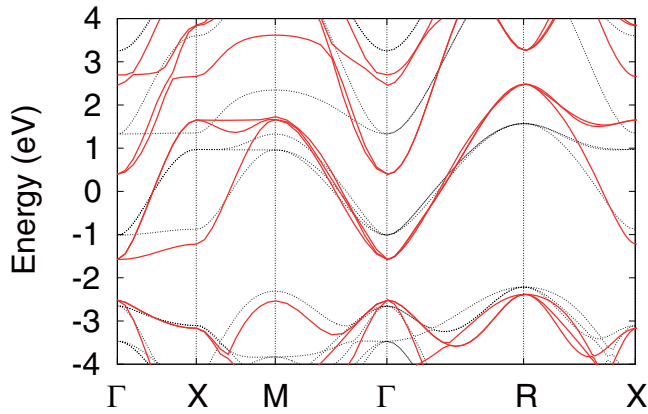
FIG. 5. Band structure of SrVO$_3$ in the Hartree approximation. For comparison, the LDA band structure is also given (black dotted line). The energy is measured from the Fermi level.

where V_{xc} is taken out, correlations within the L space are not included. The LDA, on the other hand, at least partially includes correlations within the L space, and these are very effective in narrowing the band. Interestingly, the bottom of the occupied band is quite exactly at the LDA value, and the remaining widening is purely in the unoccupied part.

To go further and in particular to analyze the dynamic behavior of $\Delta\Sigma_H$ we plot in Fig. 7 the self-energy corrections $\Delta\Sigma_H$ [with Σ, see Eq. (11) for comparison] for the real and imaginary parts at several representative choices of momenta. The frequency dependence is smooth around the Fermi level. In particular, in contrast to the full self-energy, there are no poles in $\Delta\Sigma_H$ in the low-energy region, thanks to the exclusion of fluctuations within the L space. The frequency dependence of the real part indicates that the linearization $\Delta\Sigma_H(\omega) \sim \Delta\Sigma_H(\omega=0) + [d\Delta\Sigma_H(\omega)/d\omega]_{\omega=0}\omega$ offers a reasonably good approximation. In fact, the behavior of the constrained self-energy is much closer to linearity than that of the full GW self-energy Σ. This is easily understood by the fact that the low-energy excitations are excluded in the present constrained self-energy $\Delta\Sigma_H$ analogously to an insulator, thus eliminating the strong frequency dependence
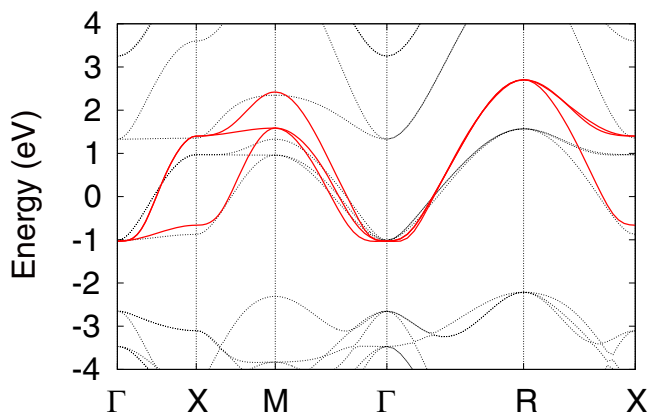
of the constrained self-energy near the Fermi level. This is one of the consequences of the controllability and an advantage of the present MACE scheme, as mentioned in the introduction. In the following discussion, we employ this linearized approximation. Then the renormalization factor Z_H defined by Eq. (22) is interpreted as that from the contribution of the H space. After this renormalization factor is taken into account, the effective Hamiltonian is given by $Z_H[H_{LDA} - V_{xc} + \Delta\Sigma_H(\omega=0)]$ (see Fig. 8). Interestingly the renormalization factor Z_H=0.92 stays close to 1, so that the bandwidth is only slightly reduced (to 3.4 eV instead of the 3.7 eV above). We also note that Z_H has weak momentum dependence as we reveal in the following.

Figure 9 shows the local and nonlocal parts of $\Delta\Sigma_H$. The frequency dependence of the local part [Figs. 9(a) and 9(b)] is quite similar to the frequency dependent self-energies at various momenta in Fig. 7. One immediately reads off an interesting property, which is akin to what has been found for the full GW self-energy in [113], namely, that the nonlocal part of $\Delta\Sigma_H$ shows only weak frequency dependence as shown in Figs. 9(c) and 9(d). This explains why Z_H is only weakly momentum dependent. On the other hand, $\Delta\Sigma_H^{nonlocal}(0)$ at R is $\sim$1 eV larger than at Γ, which causes the band widening effect. $\Delta\Sigma_H$ can thus to a good approximation be decomposed into a frequency dependent local part and a static nonlocal one: $\Delta\Sigma_H(k,\omega) = \Delta\Sigma_H^{local}(\omega) + \Delta\Sigma_H^{nonlocal}(k)$, with $\Delta\Sigma_H^{local}(\omega) = \sum_q \Delta\Sigma_H(q,\omega)$

In the simple case of SrVO$_3$, where the t$_{2g}$ states are degenerate, static local operators are scalar and are compensated by a chemical potential shift such that the correct particle number is obtained. The above band structure corresponding to $H_{LDA} - V_{xc} + \Delta\Sigma_H(k,\omega=0)$ is thus identical to that of $H_{LDA} - V_{xc} + \Delta\Sigma_H^{nonlocal}(k)$. The local dynamical part of $\Delta\Sigma_H$ then results in a narrowing of this band structure by a factor $Z_H = 0.92$.

Before turning to a discussion of the low-energy correction for the GW treatment $\Delta\Sigma_L = G^{(0)}(W - W_L)$, we analyze the effective interaction W_L shown in Fig. 10 in comparison to W and W_H. The fully screened Coulomb interaction W displays the familiar shape of an interaction that is strongly screened at low energies (with a value of 0.88 eV at $\omega = 0$), while retrieving the value of the bare Coulomb interaction v ($\sim$16.0 eV) at high energy. The crossover from the bare to the screened values takes place at the plasma energy of about 15 eV. This behavior has been discussed before [26,114]; we note in particular that the plasma frequency is known from electron energy-loss spectroscopy measurements of the related SrTiO$_3$ compound [111,115]. The partially screened interaction W_H constructed within the cRPA converges to W at high energies, but displays weaker screening effects at low energies (with a value of 3.5 eV at $\omega = 0$), since intra-t$_{2g}$ screening channels are excluded. As was already anticipated in Sec. III, W_L can be interpreted as the screened interaction of a low-energy Hamiltonian, where a static interaction of value $W_H(\omega=0)$ has been imposed as the bare interaction. Since now *only* intra-t$_{2g}$ screening channels are active, screening takes place only at low energies, where the scale is given by the t$_{2g}$ bandwidth. Also plotted is the difference $W_{GW}^{dyn} = W - W_d$: Except at low energies where the t$_{2g}$ screening channels come into play, its frequency dependence is essentially given by
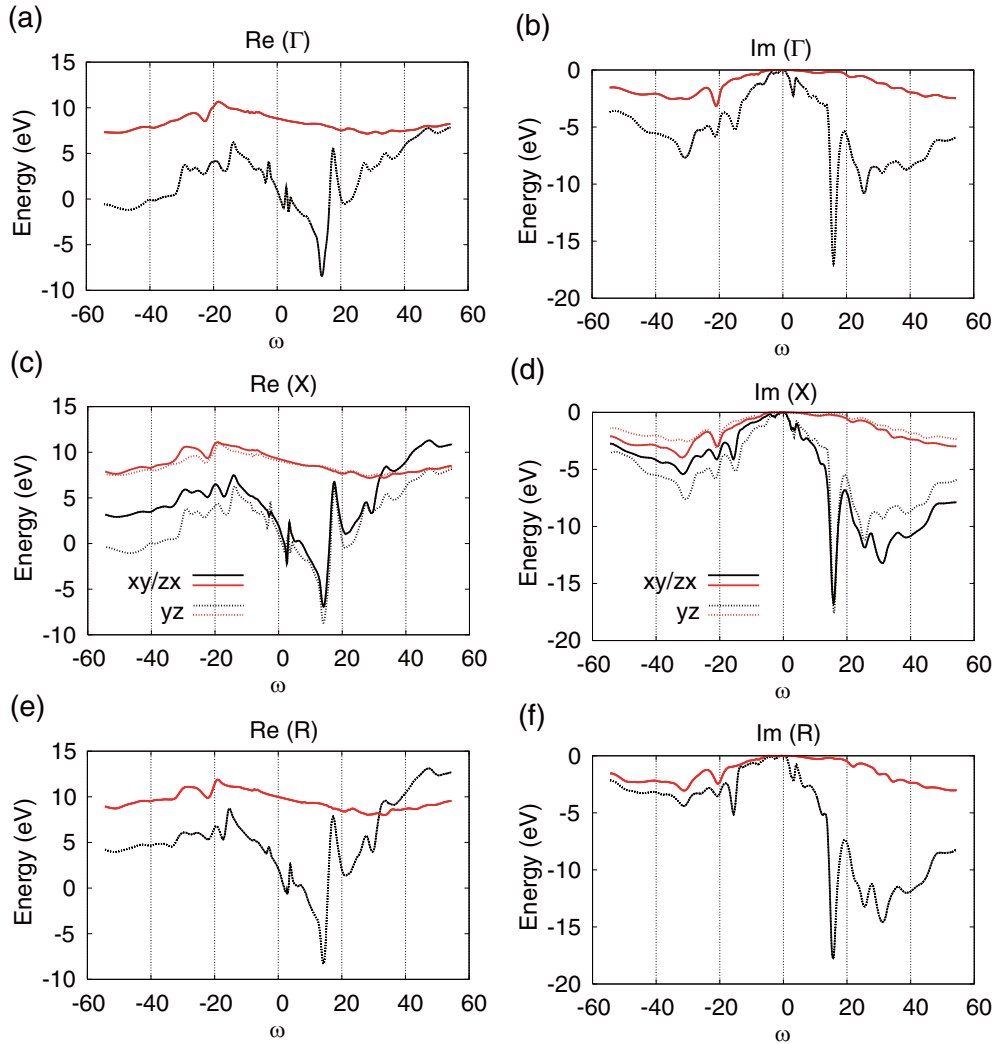

FIG. 6. Band structure of $H_{LDA} - V_{xc} + \Delta\Sigma_H(\omega=0)$ of SrVO$_3$. For comparison, the LDA band structure is also given (black dotted line). The energy is measured from the Fermi level.

FIG. 7. Frequency dependence of $-V_{xc} + \Delta\Sigma_H$ for SrVO$_3$. (a) and (b) are the real and imaginary parts at the Γ point, respectively, and (c) and (d) [(e) and (f)] are those at X (R). For comparison, the full GW self-energies are also given (black dotted line).

that of W, while the high-energy limit is the bare Coulomb interaction v reduced by $W_H(0)$.
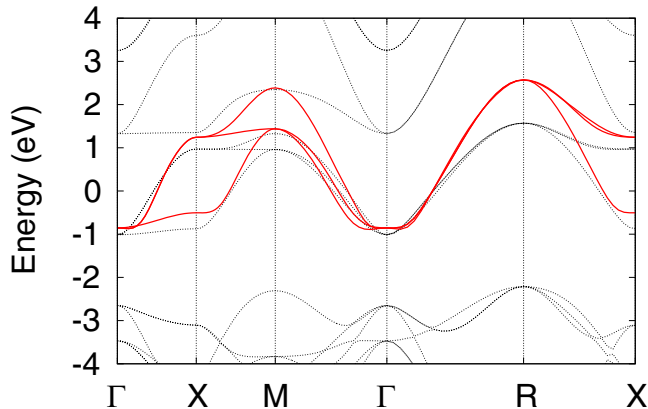

FIG. 8. Band structure of $Z_H[H_{LDA} - V_{xc} + \Delta\Sigma_H(\omega = 0)]$ of SrVO$_3$. For comparison, the LDA band structure is also given (black dotted line). The energy is measured from the Fermi level.

The frequency dependence of the real and imaginary parts of the low-energy self-energy $\Delta\Sigma_L = G^{(1)}W_H^{dyn}$ for the direct perturbative treatment is illustrated in Fig. 11. $\Delta\Sigma_L = G^{(0)}W_{GW}^{dyn}$ used for the GW treatment is shown in Fig. 12 for several choices of momenta.

The results for the perturbative and the GW treatment are nearly identical. The renormalization factor of $\Delta\Sigma_L^{nonlocal}$ (and $\Delta\Sigma_L$) is ~ 0.77. The zero-frequency shift Re$\Delta\Sigma_L^{nonlocal}(0)$ at R is ~ 3 eV larger than at Γ. Again, one sees how Σ_L separates into local dynamical and nonlocal static parts: $\Delta\Sigma_L = \Delta\Sigma_L^{nonlocal}(k) + \Delta\Sigma_L^{local}(\omega)$. This is expected since such a separation has been found within the full GW calculation [89], and is even more plausible for a GW treatment within the t$_{2g}$ subspace.

The corresponding band structures are given by $[\epsilon_{DFT} + \Delta\Sigma_H + \Delta\Sigma_L^{nonlocal}]Z_{HL}$ in Fig. 13 for the perturbative treatment [see Eq. (24)], and in Fig. 14 for the GW treatment, where $\Delta\Sigma_L^{nonlocal}$ is defined in Eq. (27) and Z_{HL} is around 0.92. Z_{HL} is practically the same as Z_H, meaning that the nonlocal dynamical correction in the H space is small, which justifies the GW perturbative treatment for the nonlocal part. One
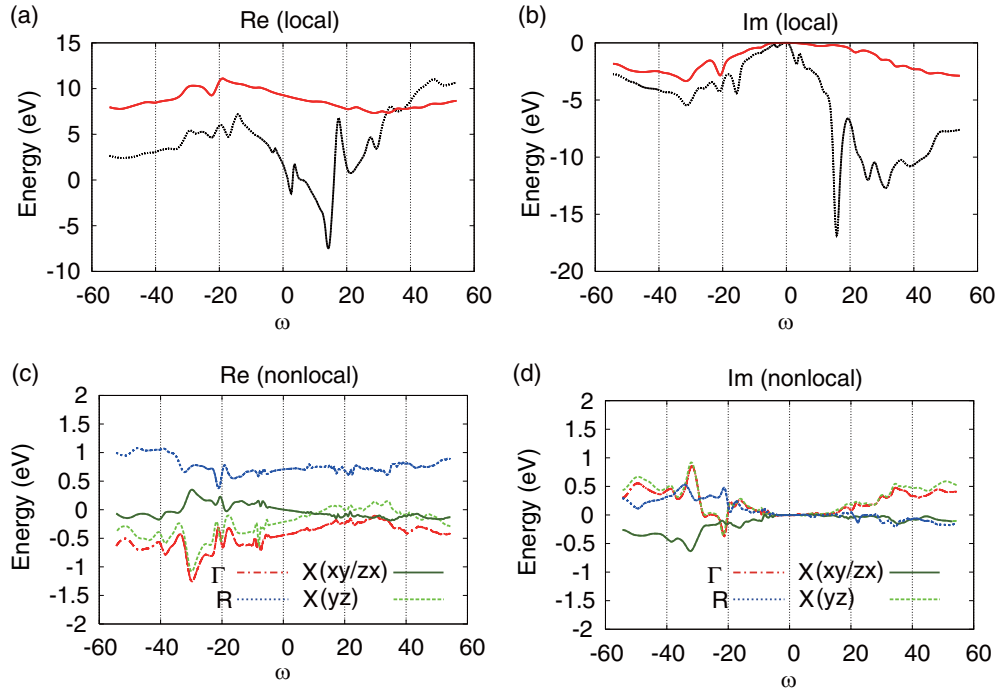
FIG. 9. Frequency dependence of $-V_{xc} + \Delta \Sigma_H$ of SrVO$_3$. (a) and (b) are the real and imaginary parts of the local component, respectively. The black dotted line is Σ defined in Eq. (11) in the full GW approximation for comparison. (c) and (d) are the real and imaginary parts at several k points.

finds that the nonlocal part $\Delta \Sigma_L = G_{ll}^{(0)}(W - W_L)$ narrows the empty states but widens the occupied ones, resulting in an overall bandwidth of 3.2 eV. The difference between the direct perturbation and the GW treatment is small.

After including the effect of the local self-energy by the nonperturbative Casula trick, we show the dispersion given by $[\epsilon_{DFT} - V_{xc} + \Delta \Sigma_H + \Delta \Sigma_L^{nonlocal}]Z_{HL}Z_B$ for the GW-type treatment in Fig. 15: The GW-like treatment gives a band dispersion close to the LDA one. The Z_B factor corresponding to the local dynamical part of $\Delta \Sigma_L$ amounts to $Z_B = 0.7$. The nonperturbative treatment results in an LDA-like band dispersion for the empty states, but a slightly narrower bandwidth in the occupied part. The low-energy effective Hamiltonian at this level of treatment has a frequency independent effective interaction both with local and nonlocal interaction given by the Fourier transform of $W_H(q,\omega = 0)$, which contains both direct and exchange interactions.

We finally show the dispersion given by Eq. (46), namely, $[\epsilon_{DFT} + \Sigma_{corr}^{GW}]Z_{corr}Z_B$ in Fig. 16. The result shows an LDA-like band dispersion for the occupied states, but a slightly wider bandwidth in the empty part, resulting in a bandwidth 14% wider in total than the LDA bandwidth. The effective interaction of the low-energy effective Hamiltonian at this final level has frequency independent local and nonlocal interactions given by the Fourier transform of $W_r(q,\omega = 0)$.

The resulting effective Hamiltonian in the L space consists of single-particle and two-particle (interaction) parts. The effective interaction is the same as in previous estimates by the cRPA in the literature, while the single-particle dispersion is revised after removing the double counting and taking into account the frequency dependence of the effective interaction. The final effective bandwidth for SrVO$_3$ is, after partial

cancellation, slightly (14%) larger than the LDA bandwidth. This is a reasonable result because the LDA takes into account all correlations though insufficiently, while the present scheme by the constrained self-energy excludes the correlation effects arising from the L space. Although the bandwidth derived for the effective Hamiltonian is slightly larger than that of the LDA, it is clear that the correlation effects are stronger than in the LDA or standard GW when the *ab initio* Hamiltonian is solved by an accurate solver. In fact, if the effective interaction contained in the final effective Hamiltonian is treated by the GW scheme, one obtains the dispersion illustrated in Fig. 17, which is given from the self-energy of the whole GW calculation Σ by correcting the local dynamical part $W - W_L$ by Z_B. This indicates that even an insufficient treatment of the local static interaction by the GW scheme gives a dispersion with the bandwidth ($\sim$1.9 eV) narrower than the LDA ($\sim$2.5 eV, Fig. 2) and GW ($\sim$2.1 eV, Fig. 3) dispersions. A slightly ($\sim$14%) wider dispersion than that of the LDA bands obtained for the effective Hamiltonian accompanied with frequency independent effective Coulomb interactions without the exchange part may account for the slight overestimate of correlation effects in the literature mentioned in the introduction. Our scheme offers an optimized way for the derivation of *ab initio* Hamiltonians for the L space after eliminating the H space in a systematic fashion.

Our findings of the band widening are consistent with studies based on the combined GW+DMFT method in the literature [89]: There, it was argued that within GW+DMFT the best effective Hamiltonian that DMFT should be performed on is a one-body Hamiltonian corrected by the nonlocal part of the GW self-energy. The corresponding spectral function (see, e.g., Fig. 5 of [89]) displays a broadening similar to
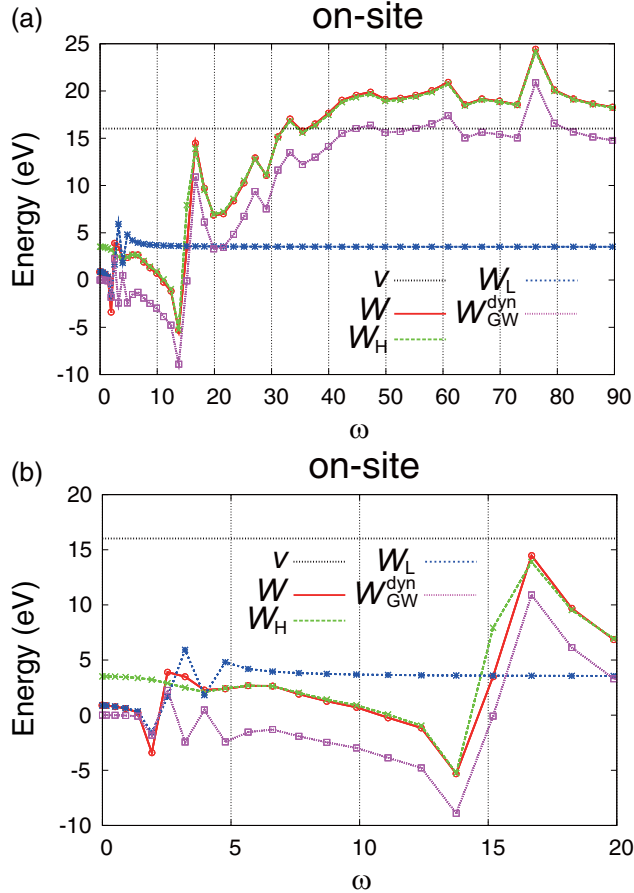
FIG. 10. (a) Frequency dependence of the on-site effective interaction. Panel (b) is a low-energy zoom of panel (a).

Fig. 14. Most interestingly, our present calculations confirm a pronounced asymmetry observed in [89], namely, a stronger widening effect in the unoccupied part of the spectrum than in the occupied one. We will come back to this point below.

VIII. TEST OF THE EFFECTIVE HAMILTONIAN: DYNAMICAL MEAN FIELD THEORY FOR SrVO₃

To validate our effective Hamiltonian construction, we close the paper by presenting a dynamical mean field solution of the final Hamiltonian (45). In Fig. 18, we plot the spectral function in comparison to the density of states for a noninteracting effective Hamiltonian. Also superposed are the photoemission data of [96].

Several remarks are in order. First, we note that while the effective Hamiltonian has a larger overall bandwidth than the DFT-LDA band structure, as discussed above (and already visible from Fig. 16), the widening is taking place on the unoccupied part of the spectrum, while the bottom of the t_{2g} band is even slightly higher in energy (that is, closer to the Fermi level) than in the LDA. At given interaction strength, we therefore expect the effective Hamiltonian to have a smaller kinetic energy and thus a higher correlation strength than the LDA. This expectation is verified: DFT+DMFT calculations with a Hubbard U as small as the zero-frequency value of the cRPA $U(\omega)$ are known to display only a minor band

renormalization accompanied by a slight "washing out" of spectral weight to higher energies, but no true Hubbard band. The DMFT solution of the effective Hamiltonian is slightly more correlated in that a Hubbard-type shoulder appears around -1 to -1.5 eV binding energy.

At first sight, the comparison to the experimental data seems to be unfavorable, since in photoemission experiments a much stronger peak is generally observed at the energy corresponding to the expected lower Hubbard band. This conclusion would, however, be too quick. Indeed, as shown recently [116], a substantial part of the spectral weight found at these energies in photoemission spectra is due to the presence of oxygen vacancies in the sample. In the light of these findings, our data are fully compatible with the experimental measurement.

On the unoccupied side of the spectrum, the situation is even more interesting. Here, the early DMFT literature was interpreting a pronounced peak at about 2.7 eV seen in *Bremsstrahlisochromat* spectroscopy (BIS) as the upper Hubbard band of t_{2g} character. This interpretation was, however, questioned in [88], on the basis of GW+DMFT calculations, proposing a reinterpretation as e_g-dominated spectral weight. The more recent literature [89,110] is consistent with this reinterpretation.

The DMFT calculation based on the present effective Hamiltonian renormalizes the overall bandwidth (compare the solid line to the points in Fig. 18); the corresponding spectral weight is shifted to higher energies but merely as an extended high-frequency tail. No upper Hubbard band is observed. Even more interestingly, the quasiparticle part of the spectral functions mimics in a very clear fashion the shape of the underlying noninteracting density of states, displaying a pronounced peak around 0.8 eV. In comparison with the spectral functions found in [88], these findings might even imply interesting suggestions for the interpretation of the GW+DMFT spectral function: Indeed, in the GW+DMFT calculations a broad extended quasiparticle peak was observed, and it was speculated that an upper Hubbard band, if present, would be merged into the large central peak. The present findings rather suggest that peak to result from weakly renormalized quasiparticle states, retaining roughly the shape of the noninteracting band.

The present DMFT calculation thus validates our effective Hamiltonian construction. Most importantly, we stress that it incorporates nontrivial effects beyond standard DFT+DMFT, which are also present in more refined GW+DMFT calculations [88,89].

IX. SUMMARY AND CONCLUSION

In this paper, we have developed and elaborated a method for a truly first-principles electronic description of correlated electron materials. Conceptually speaking, the scheme is based on RG arguments, which guarantee the existence of an effective Hamiltonian valid at a given energy scale. The difficulty consists, however, in determining this Hamiltonian explicitly, since a direct quantitative RG treatment of the full Coulomb Hamiltonian is a very difficult task and has not been achieved so far. Indeed, performing RG calculations with long-range interactions in the continuum is an even more
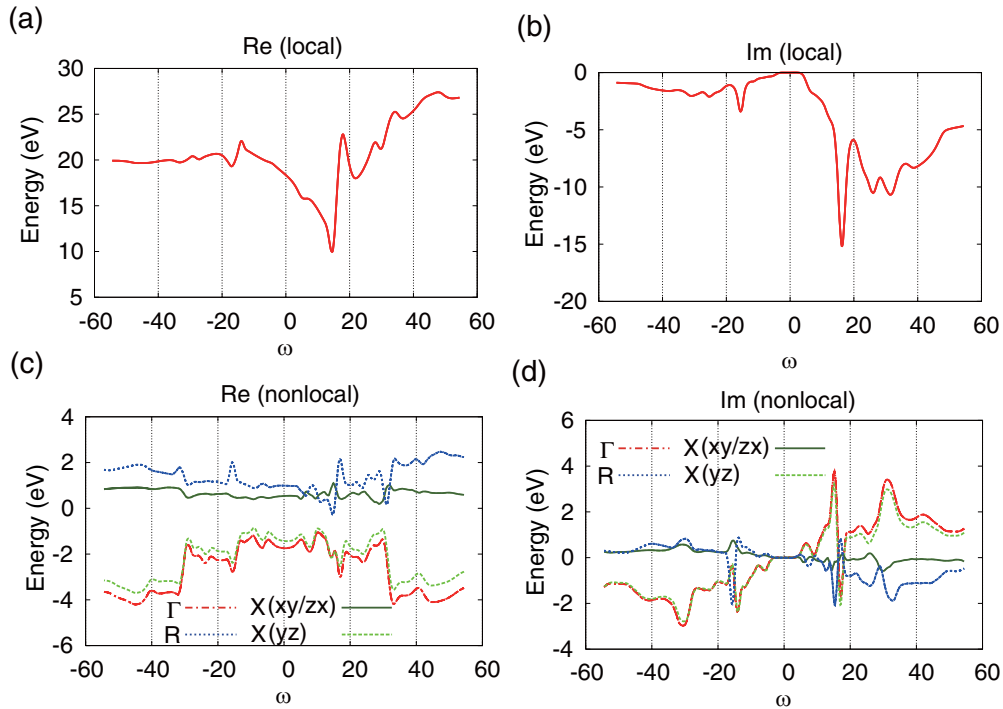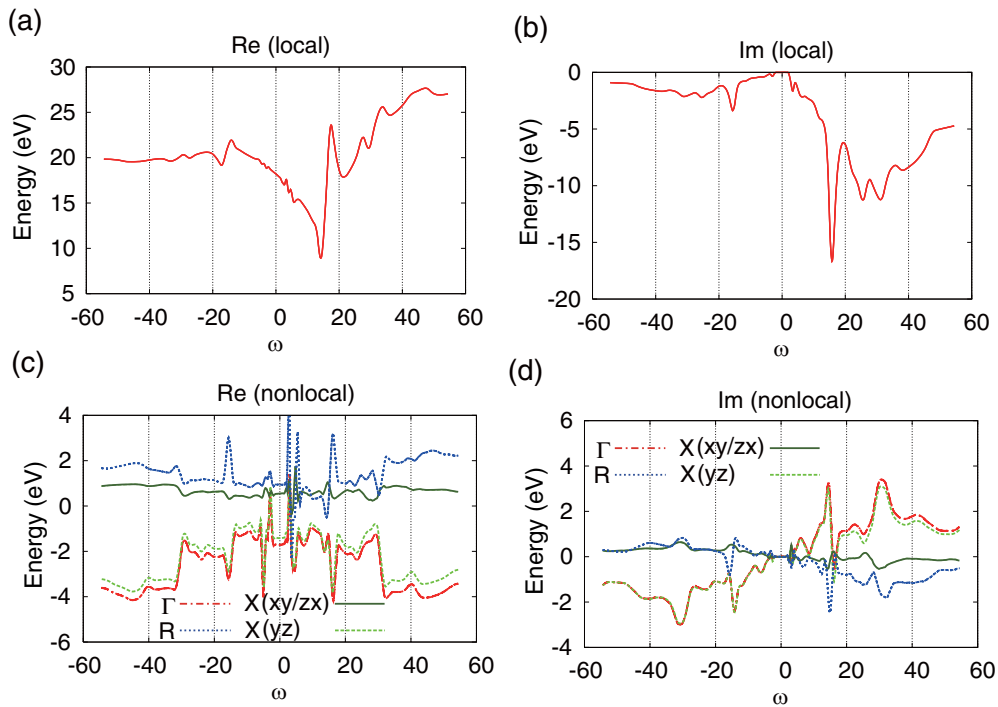
FIG. 11. Frequency dependence of $-V_{xc} + G^{(1)} W_H^{dyn}$ of SrVO$_3$. (a) and (b) are the real and imaginary local parts, respectively. (c) and (d) are the real and imaginary parts at several k points.

difficult task than for simplified models [117], and even for interacting lattice models explicit RG calculations remain a challenge.

Our scheme proposes an indirect way of constructing the low-energy Hamiltonian which can be considered a shortcut to a true RG treatment. The RG has to satisfy the chain rule, where the full trace summation denoted by $\mathcal{R}$ can be decomposed into the two subsequent partial trace operations $\mathcal{R}_H \mathcal{R}_L$ as required for a semigroup. The first operation $\mathcal{R}_H$ can be replaced by a perturbative treatment in a controlled approximation, thanks

FIG. 12. Frequency dependence of $-V_{xc} + G^{(0)} W_{GW}^{dyn}$ of SrVO$_3$. (a) and (b) are the real and imaginary local parts, respectively. (c) and (d) are the real and imaginary parts at several k points.
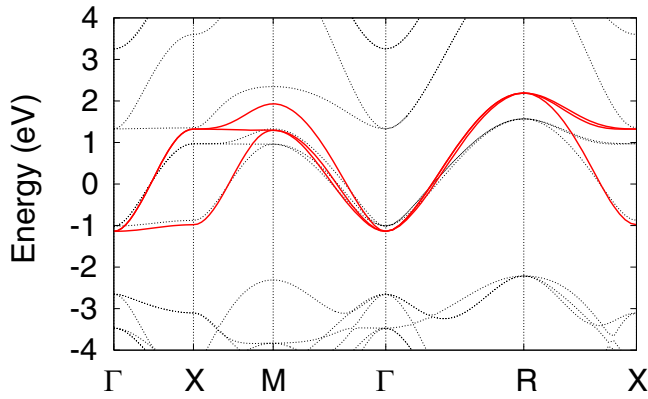
FIG. 13. Band structure of $[\epsilon_{\mathrm{DFT}} - V_{\mathrm{xc}} + \Delta\Sigma_{\mathrm{H}} + \Delta\Sigma_{\mathrm{L}}^{\mathrm{nonlocal}}]Z_{\mathrm{HL}}$ of $SrVO_3$ in the direct perturbative treatment. For comparison, the LDA band structure is also given (black dotted line). The energy is measured from the Fermi level.

FIG. 15. Band structure of $[\epsilon_{\mathrm{DFT}} - V_{\mathrm{xc}} + \Delta\Sigma_{\mathrm{H}} + \Delta\Sigma_{\mathrm{L}}^{\mathrm{nonlocal}}]Z_{\mathrm{HL}}Z_B$ of $SrVO_3$ in the GW treatment. For comparison, the LDA band structure is also given (black dotted line). The energy is measured from the Fermi level.

to the separation of the L and H spaces. Then the idea can be understood as working one's way backwards, starting from the full solution obtained within some approximation (here, perturbation theory). The desired low-energy Hamiltonian is constructed such as to fulfill the following requirement: its solution within the same approximation applied to the low-energy subspace only should yield the same result as the projection of the full solution to that subspace. The motivation of this constructions resides in the fact that instead of solving the resulting low-energy Hamiltonian within the approximation used for its construction more accurate many-body solvers can be used for the final solution.

Strongly correlated electron systems provide a natural ground for such a treatment, due to their hierarchical structure in energy space, which facilitates the identification of appropriate low-energy windows. Nevertheless, in practice, the explicit construction of accurate low-energy effective Hamiltonians has remained a challenge due to the difficulties associated to bridging the description of the high-energy degrees of freedom usually treated in the DFT and the low-energy degrees of freedom described by the effective Hamiltonian in a consistent
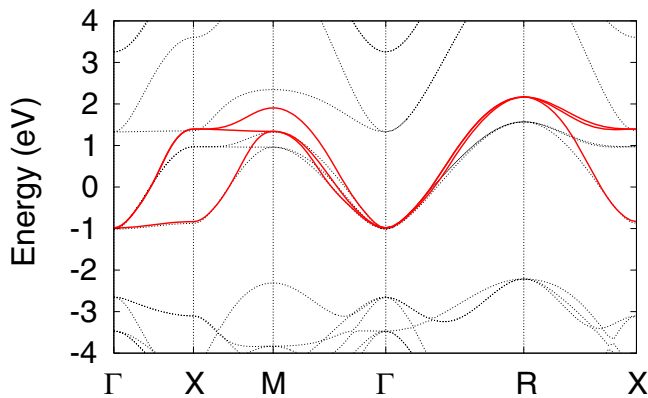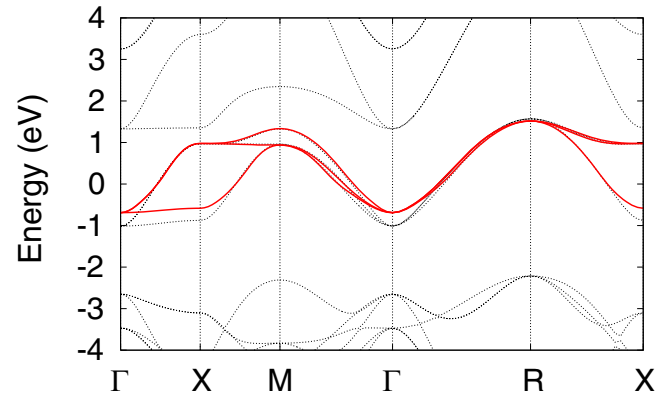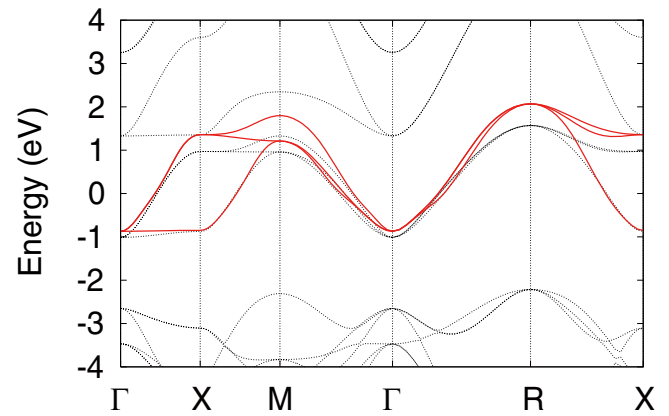

FIG. 16. Band structure of $[\epsilon_{\mathrm{DFT}} + \Sigma_{\mathrm{corr}}^{GW}]Z_{\mathrm{corr}}Z_B$ of $SrVO_3$. For comparison, the LDA band structure is also given (black dotted line). The energy is measured from the Fermi level.
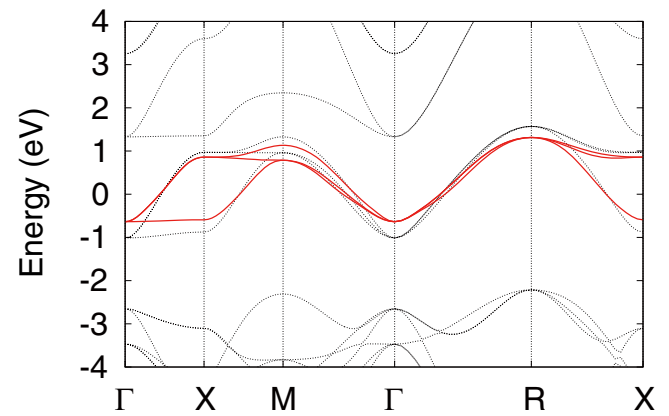

FIG. 14. Band structure of $[\epsilon_{\mathrm{DFT}} - V_{\mathrm{xc}} + \Delta\Sigma_{\mathrm{H}} + \Delta\Sigma_{\mathrm{L}}^{\mathrm{nonlocal}}]Z_{\mathrm{HL}}$ of $SrVO_3$ in the GW treatment. For comparison, the LDA band structure is also given (black dotted line). The energy is measured from the Fermi level.

FIG. 17. Band structure of $[\epsilon_{\mathrm{DFT}} - V_{\mathrm{xc}} + \Sigma - (G^{(0)}W_{GW}^{\mathrm{dyn}})^{\mathrm{nonlocal}}]Z'Z_B$ of $SrVO_3$ [Z' is the renormalization factor of $\Sigma - (G^{(0)}W_{GW}^{\mathrm{dyn}})^{\mathrm{nonlocal}}$]. For comparison, the LDA band structure is also given (black dotted line). The energy is measured from the Fermi level.
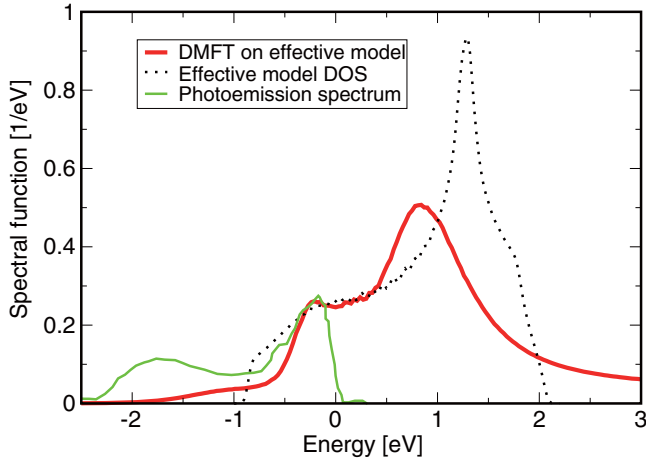
FIG. 18. Dynamical mean field solution of the final effective Hamiltonian Eq. (45) [Fig. (16)]. The resulting spectral function [for static interactions $U(0) = 3$ eV, $J = 0.6$, and inverse temperature $\beta = 10$ eV^{-1}] (thick solid line) as compared to the noninteracting density of states of the effective Hamiltonian (points) and the photoemission spectrum of Ref. [96] (thin solid line).

manner. The main obstacles are related to (1) the need of avoiding double counting of correlations and screening in the high- and low-energy treatments and (2) the frequency dependence of parameters in the low-energy effective models.

In this paper, we have presented a way to overcome these bottlenecks: we propose a systematic recipe for how a low-energy Hamiltonian can be constructed by starting from a perturbative treatment. We provide the best description under the constraint that the effective low-energy Hamiltonian contains only single-particle (kinetic-energy term) and two-particle (interaction energy) terms with frequency independent parameters. Our construction relies on a controlled perturbative treatment, which is possible thanks to the hierarchical nature of correlated electron systems: Even in cases where perturbation theory would not provide a meaningful approximation to the full problem, a perturbative treatment of the high-energy degrees of freedom only can be justified thanks to the fact that quantum many-body fluctuations primarily live in the low-energy space only.

On the example of the ternary transition-metal compound SrVO$_3$, we have explicitly demonstrated how this construction works: A low-energy Hamiltonian is built in such a way that a perturbative treatment would reproduce the result of a perturbative treatment in the full space as closely as possible. Solving the resulting many-body Hamiltonian within accurate nonperturbative many-body solvers then provides a description beyond the perturbative treatment, while still keeping the *ab initio* nature of the calculation. We have tested our scheme in a step-by-step manner, identifying the effects of the different corrective terms. Most interestingly, our results confirm recent findings within GW+DMFT calculations on SrVO$_3$ which identified an intriguing asymmetry in the corrections to an LDA Hamiltonian [89]. Our substantially improved MACE scheme should thus open new ways to accurate many-body calculations beyond current *ab initio* methods.

If the bands are entangled rather than isolated near the Fermi energy, in principle one needs to include all the entangled bands near the Fermi level. For moderately entangled cases, the reader is referred to the disentanglement procedure described in [118]. If the separation of the bands near the Fermi level is not complete, feedback effects from the nearby degrees of freedom have to be taken into account self-consistently, which requires an extension of the present framework left for future study.

Note added. While this paper was under review, another refined GW+DMFT study [119] appeared, which is also consistent with the interpretation of the BIS peak as e$_g$ density of states. In the occupied part, there is at most a weak Hubbard shoulder, in agreement with the present paper.

APPENDIX

In this Appendix, we analyze the difference between the local GW self-energy

$$\Sigma_{\text{loc}} = G_{\text{loc}} W_{\text{loc}} \tag{A1}$$

and the GW self-energy obtained from a local W.

We use the expansions

$$G(r, r') = \sum_{RR'LL'} G_{RR'LL'} \chi_{RL}(r) \chi_{R'L'}(r') \tag{A2}$$

and

$$W(r, r') = \sum_{RR'\alpha\beta} W_{RR'\alpha\beta} B_{R\alpha}(r) B_{R'\beta}(r') \tag{A3}$$

on the one- and two-particle bases χ and B, respectively (following standard notations in the field). Then, the GW equation

$$\Sigma(r, r') = G(r, r') W(r, r') \tag{A4}$$

leads to

$$\Sigma_{R_1 R_2 L_1 L_2} = \sum_{RR'LL'} \sum_{\tilde{R}\tilde{R}'\alpha\beta} G_{RR'LL'} W_{\tilde{R}\tilde{R}'\alpha\beta}$$
$$\times \langle \chi_{R_1 L_1} \chi_{RL} | B_{\tilde{R}'\alpha} \rangle \langle B_{\tilde{R}\beta} | \chi_{R_2 L_2} \chi_{R'L'} \rangle. \tag{A5}$$

For a local W, that is, an interaction of the form $W_{\tilde{R}\tilde{R}'\alpha\beta} \sim \delta_{RR'}$, one has

$$\Sigma_{R_1R_2L_1L_2} = \sum_{RR'LL'}\sum_{\tilde{R}\alpha\beta} G_{RR'LL'}W_{\tilde{R}\tilde{R}\alpha\beta}$$
$$\times \langle\chi_{R_1L_1}\chi_{RL}|B_{\tilde{R}\alpha}\rangle\langle B_{\tilde{R}\beta}|\chi_{R_2L_2}\chi_{R'L'}\rangle. \quad (A6)$$

The structure of this equation is determined by the overlap matrices of two-particle and one-particle basis states. If the basis set is sufficiently localized that no overlaps between basis

functions on different spheres need to be considered, these become local quantities themselves: $O_{L_1L\alpha} = \langle\chi_{RL_1}\chi_{RL}|B_{R\alpha}\rangle$ and the above expression equals the local self-energy

$$\Sigma_{RRL_1L_2} = \sum_{LL'}\sum_{\alpha\beta} G_{RRLL'}W_{RR\alpha\beta}$$
$$\times \langle\chi_{RL_1}\chi_{RL}|B_{R\alpha}\rangle\langle B_{R\beta}|\chi_{RL_2}\chi_{RL'}\rangle. \quad (A7)$$

This is used in order to write Eq. (26).

[1] M. Imada, A. Fujimori, and Y. Tokura, Rev. Mod. Phys. **70**, 1039 (1998).

[2] W. Kohn, Rev. Mod. Phys. **71**, 1253 (1999).

[3] F. Aryasetiawan and O. Gunnarsson, Rep. Prog. Phys. **61**, 237 (1998).

[4] M. Imada and T. Miyake, J. Phys. Soc. Jpn. **79**, 112001 (2010).

[5] S. Biermann, *"LDA+DMFT"—A Tool for Investigating the Electronic Structure of Materials with Strong Electronic Coulomb Correlations, Encyclopedia of Materials: Science and Technology* (Elsevier, Amsterdam, 2005); *Dynamical Mean Field-Based Electronic Structure Calculations for Correlated Materials, First Principles Approaches to Spectroscopic Properties of Complex Materials, Topics in Current Chemistry* (Springer, Berlin, 2014).

[6] G. Kotliar, S. Y. Savrasov, K. Haule, V. S. Oudovenko, O. Parcollet, and C. A. Marianetti, Rev. Mod. Phys. **78**, 865 (2006).

[7] S. R. White and R. L. Martin, J. Chem. Phys. **110**, 4127 (1999).

[8] Y. Kurashige and T. Yanai, J. Chem. Phys. **130**, 234114 (2009).

[9] M. Casula, C. Attaccalite, and S. Sorella, J. Chem. Phys. **121**, 7110 (2004).

[10] P. Navratil, S. Quaglioni, I. Stetcu, and B. R. Barrett, J. Phys. G **36**, 083101 (2009).

[11] G. Hagen, T. Papenbrock, D. J. Dean, and M. Hjorth-Jensen, Phys. Rev. C **82**, 034330 (2010).

[12] F. Aryasetiawan, M. Imada, A. Georges, G. Kotliar, S. Biermann, and A. I. Lichtenstein, Phys. Rev. B **70**, 195104 (2004).

[13] T. Miyake and F. Aryasetiawan, Phys. Rev. B **77**, 085122 (2008).

[14] L. Vaugier, H. Jiang, and S. Biermann, Phys. Rev. B **86**, 165105 (2012).

[15] R. Thomale, C. Platt, W. Hanke, J. P. Hu, and B. A. Bernevig, Phys. Rev. Lett. **107**, 117001 (2011).

[16] C. Platt, W. Hanke, and R. Thomale, Adv. Phys. **62**, 453 (2013).

[17] T. Kashima and M. Imada, J. Phys. Soc. Jpn. **70**, 2287 (2001).

[18] K. A. Hallberg, Adv. Phys. **55**, 477 (2006).

[19] B. Edegger, V. N. Muthukumar, and C. Gros, Adv. Phys. **56**, 927 (2007).

[20] D. Tahara and M. Imada, J. Phys. Soc. Jpn. **77**, 114701 (2008).

[21] A. Georges, G. Kotliar, W. Krauth, and M. J. Rozenberg, Rev. Mod. Phys. **68**, 13 (1996).

[22] T. Maier, M. Jarrell, T. Pruschke, and M. H. Hettler, Rev. Mod. Phys. **77**, 1027 (2005).

[23] K. Held, O. K. Andersen, M. Feldbacher, A. Yamasaki, and Y.-F. Yang, J. Phys.: Condens. Matter **20**, 064202 (2008).

[24] V. I. Anisimov, A. I. Poteryaev, M. A. Korotin, A. O. Anokhin, and G. Kotliar, J. Phys.: Condens. Matter **9**, 7359 (1997).

[25] A. I. Lichtenstein and M. I. Katsnelson, Phys. Rev. B **57**, 6884 (1998).

[26] S. Biermann, J. Phys.: Condens. Matter **26**, 173202 (2014).

[27] S. Biermann, A. Dallmeyer, C. Carbone, W. Eberhardt, C. Pampuch, O. Rader, M. I. Katsnelson, and A. I. Lichtenstein, JETP Lett. **80**, 612 (2004); arXiv:cond-mat/0112430.

[28] A. I. Lichtenstein, M. I. Katsnelson, and G. Kotliar, Phys. Rev. Lett. **87**, 067205 (2001).

[29] I. V. Solovyev and M. Imada, Phys. Rev. B **71**, 045103 (2005).

[30] J. Braun, J. Minar, H. Ebert, M. I. Katsnelson, and A. I. Lichtenstein, Phys. Rev. Lett. **97**, 227601 (2006).

[31] J. Sanchez-Barriga, J. Braun, J. Minar, I. Di Marco, A. Varykhalov, O. Rader, V. Boni, V. Bellini, F. Manghi, H. Ebert, M. I. Katsnelson, A. I. Lichtenstein, O. Eriksson, W. Eberhardt, H. A. Durr, and J. Fink, Phys. Rev. B **85**, 205109 (2012).

[32] Y. Imai, I. Solovyev, and M. Imada, Phys. Rev. Lett. **95**, 176405 (2005).

[33] Y. Imai and M. Imada, J. Phys. Soc. Jpn. **75**, 094713 (2006).

[34] Y. Otsuka and M. Imada, J. Phys. Soc. Jpn. **75**, 124707 (2006).

[35] S. Biermann, A. Poteryaev, A. I. Lichtenstein, and A. Georges, Phys. Rev. Lett. **94**, 026404 (2005); J. M. Tomczak and S. Biermann, J. Phys.: Condens. Matter **19**, 365206 (2007); Europhys. Lett. **86**, 37004 (2009); Phys. Rev. B **80**, 085117 (2009); J. M. Tomczak, F. Aryasetiawan, and S. Biermann, *ibid.* **78**, 115103 (2008).

[36] F. Aryasetiawan, J. M. Tomczak, T. Miyake, and R. Sakuma, Phys. Rev. Lett. **102**, 176402 (2009).

[37] P. Thunstrom, I. Di Marco, and O. Eriksson, Phys. Rev. Lett. **109**, 186401 (2012).

[38] A. I. Poteryaev, J. M. Tomczak, S. Biermann, A. Georges, A. I. Lichtenstein, A. N. Rubtsov, T. Saha-Dasgupta, and O. K. Andersen, Phys. Rev. B **76**, 085127 (2007); J. M. Tomczak and S. Biermann, J. Phys.: Condens. Matter **21**, 064209 (2009).

[39] F. Lechermann, S. Biermann, and A. Georges, Phys. Rev. Lett. **94**, 166402 (2005); Phys. Rev. B **76**, 085101 (2007).

[40] K. Nakamura, R. Arita, and M. Imada, J. Phys. Soc. Jpn. **77**, 093711 (2008).

[41] M. Aichhorn, L. Pourovskii, V. Vildosola, M. Ferrero, O. Parcollet, T. Miyake, A. Georges, and S. Biermann, Phys. Rev. B **80**, 085101 (2009).

[42] T. Miyake, K. Nakamura, R. Arita, and M. Imada, J. Phys. Soc. Jpn. **79**, 044705 (2010).

[43] M. Aichhorn, S. Biermann, T. Miyake, A. Georges, and M. Imada, Phys. Rev. B **82**, 064504 (2010).

[44] T. Misawa, K. Nakamura, and M. Imada, J. Phys. Soc. Jpn. **80**, 023704 (2011).

[45] Z. P. Yin, K. Haule, and G. Kotliar, Nat. Mat. **10**, 932 (2011).

[46] T. Misawa, K. Nakamura, and M. Imada, Phys. Rev. Lett. **108**, 177007 (2012).

[47] T. Misawa and M. Imada, Nat. Commun. **5**, 5738 (2014).

[48] J. Ma, A. van Roekeghem, P. Richard, Z. Liu, H. Miao, L. Zeng, N. Xu, M. Shi, C. Cao, J. He, G. Chen, Y. Sun, G. Cao, S. Wang, S. Biermann, T. Qian, and H. Ding, Phys. Rev. Lett. **113**, 266407 (2014).

[49] B. Amadon, S. Biermann, A. Georges, and F. Aryasetiawan, Phys. Rev. Lett. **96**, 066402 (2006).

[50] J. Bieder and B. Amadon, Phys. Rev. B **89**, 195132 (2014).

[51] N. Devaux, M. Casula, F. Decremps, and S. Sorella, Phys. Rev. B **91**, 081101(R) (2015).

[52] L. V. Pourovskii, B. Amadon, S. Biermann, and A. Georges, Phys. Rev. B **76**, 235101 (2007).

[53] L. Pourovskii, V. Vildosola, S. Biermann, and A. Georges, Europhys. Lett. **84**, 37006 (2008).

[54] T. Miyake, L. Pourovskii, V. Vildosola, S. Biermann, and A. Georges, J. Phys. Soc. Jpn. **77**(Suppl. C), 99 (2008).

[55] J. M. Tomczak, L. V. Pourovskii, L. Vaugier, A. Georges, and S. Biermann, Proc. Natl. Acad. Sci. USA **110**, 904 (2013).

[56] H. C. Choi, B. I. Min, J. H. Shim, K. Haule, and G. Kotliar, Phys. Rev. Lett. **108**, 016402 (2012).

[57] L. V. Pourovskii, P. Hansmann, M. Ferrero, and A. Georges, Phys. Rev. Lett. **112**, 106407 (2014).

[58] S. Savrasov, G. Kotliar, and E. Abrahams, Nature (London) **410**, 793 (2001).

[59] L. V. Pourovskii, G. Kotliar, M. I. Katsnelson, and A. I. Lichtenstein, Phys. Rev. B **75**, 235107 (2007).

[60] S. Y. Savrasov, K. Haule, and G. Kotliar, Phys. Rev. Lett. **96**, 036404 (2006).

[61] J. Kolorenč, A. B. Shick, and A. I. Lichtenstein, Phys. Rev. B **92**, 085125 (2015).

[62] K. Nakamura, Y. Yoshimoto, T. Kosugi, R. Arita, and M. Imada, J. Phys. Soc. Jpn. **78**, 083710 (2009).

[63] K. Nakamura, Y. Yoshimoto, and M. Imada, Phys. Rev. B **86**, 205117 (2012).

[64] H. Shinaoka and M. Imada, J. Phys. Soc. Jpn. **81**, 034701 (2012).

[65] J. Ferber, K. Foyevtsova, H. O. Jeschke, and R. Valenti, arXiv:1209.4466.

[66] K. Nakamura, Y. Yoshimoto, R. Arita, S. Tsuneyuki, and M. Imada, Phys. Rev. B **77**, 195126 (2008).

[67] J. M. Tomczak, K. Haule, T. Miyake, A. Georges, and G. Kotliar, Phys. Rev. B **82**, 085104 (2010).

[68] C. Martins, M. Aichhorn, L. Vaugier, and S. Biermann, Phys. Rev. Lett. **107**, 266404 (2011).

[69] C. Martins, M. Aichhorn, and S. Biermann (unpublished).

[70] R. Arita, J. Kunes, A. V. Kozhevnikov, A. G. Eguiluz, and M. Imada, Phys. Rev. Lett. **108**, 086403 (2012).

[71] Y. Yamaji, Y. Nomura, M. Kurita, R. Arita, and M. Imada, Phys. Rev. Lett. **113**, 107201 (2014).

[72] M. Hirayama, T. Miyake, and M. Imada, J. Phys. Soc. Jpn. **81**, 084708 (2012).

[73] P. Hansmann, L. Vaugier, H. Jiang, and S. Biermann, J. Phys.: Condens. Matter **25**, 094005 (2013).

[74] K. Nakamura, Y. Yoshimoto, Y. Nohara, and M. Imada, J. Phys. Soc. Jpn. **79**, 123708 (2010).

[75] P. Werner, M. Casula, T. Miyake, F. Aryasetiawan, A. J. Millis, and S. Biermann, Nat. Phys. **8**, 331 (2012).

[76] M. Casula, P. Werner, L. Vaugier, F. Aryasetiawan, T. Miyake, A. J. Millis, and S. Biermann, Phys. Rev. Lett. **109**, 126408 (2012).

[77] M. Hirayama, T. Misawa, T. Miyake, and M. Imada, J. Phys. Soc. Jpn. **84**, 093703 (2015).

[78] A. van Roekeghem, T. Ayral, J. M. Tomczak, M. Casula, N. Xu, H. Ding, M. Ferrero, O. Parcollet, H. Jiang, and S. Biermann, Phys. Rev. Lett. **113**, 266403 (2014).

[79] S. Biermann, F. Aryasetiawan, and A. Georges, Phys. Rev. Lett. **90**, 086402 (2003).

[80] A. van Roekeghem and S. Biermann, Europhys. Lett. **108**, 57003 (2014).

[81] J. Lee and K. Haule, Phys. Rev. B **91**, 155144 (2015); K. Haule, Phys. Rev. Lett. **115**, 196403 (2015).

[82] M. Hirayama, T. Miyake, and M. Imada, Phys. Rev. B **87**, 195144 (2013).

[83] M. Casula, A. Rubtsov, and S. Biermann, Phys. Rev. B **85**, 035115 (2012).

[84] P. Werner, R. Sakuma, F. Nilsson, and F. Aryasetiawan, Phys. Rev. B **91**, 125142 (2015).

[85] A. van Roekeghem, P. Richard, X. Shi, S. Wu, L. Zeng, B. Saparov, Y. Ohtsubo, T. Qian, A. S. Sefat, S. Biermann, and H. Ding, Phys. Rev. B **93**, 245139 (2016).

[86] R. Sakuma, P. Werner, and F. Aryasetiawan, Phys. Rev. B **88**, 235110 (2013).

[87] R. Sakuma, C. Martins, T. Miyake, and F. Aryasetiawan, Phys. Rev. B **89**, 235119 (2014).

[88] J. M. Tomczak, M. Casula, T. Miyake, F. Aryasetiawan, and S. Biermann, Europhys. Lett. **100**, 67001 (2012).

[89] J. M. Tomczak, M. Casula, T. Miyake, and S. Biermann, Phys. Rev. B **90**, 165138 (2014).

[90] As above, if partial self-consistency is preferred, one may replace $G_{ll}^{(0)}$ with $G_{ll}^{(2)}$.

[91] I. G. Lang and Y. A. Firsov, Sov. Phys. JETP **16**, 1301 (1962).

[92] P. Sun and G. Kotliar, Phys. Rev. Lett. **92**, 196402 (2004).

[93] T. Ayral, P. Werner, and S. Biermann, Phys. Rev. Lett. **109**, 226401 (2012).

[94] E. Pavarini, S. Biermann, A. Poteryaev, A. I. Lichtenstein, A. Georges, and O. K. Andersen, Phys. Rev. Lett. **92**, 176403 (2004).

[95] F. Lechermann, A. Georges, A. Poteryaev, S. Biermann, M. Posternak, A. Yamasaki, and O. K. Andersen, Phys. Rev. B **74**, 125120 (2006).

[96] A. Sekiyama, H. Fujiwara, S. Imada, S. Suga, H. Eisaki, S. I. Uchida, K. Takegahara, H. Harima, Y. Saitoh, I. A. Nekrasov, G. Keller, D. E. Kondakov, A. V. Kozhevnikov, T. Pruschke, K. Held, D. Vollhardt, and V. I. Anisimov, Phys. Rev. Lett. **93**, 156402 (2004).

[97] I. Inoue, H. Makino, I. Hase, M. Ishikawa, N. Hussey, and M. Rozenberg, Physica B: Condens. Matter **237-238**, 61 (1997).

[98] K. Maiti, D. D. Sarma, M. J. Rozenberg, I. H. Inoue, H. Makino, O. Goto, M. Pedio, and R. Cimino, Europhys. Lett. **55**, 246 (2001).

[99] K. Maiti, U. Manju, S. Ray, P. Mahadevan, I. H. Inoue, C. Carbone, and D. D. Sarma, Phys. Rev. B **73**, 052508 (2006).

[100] M. Takizawa, M. Minohara, H. Kumigashira, D. Toyota, M. Oshima, H. Wadati, T. Yoshida, A. Fujimori, M. Lippmaa,

M. Kawasaki, H. Koinuma, G. Sordi, and M. Rozenberg, Phys. Rev. B **80**, 235104 (2009).

[101] T. Yoshida, M. Hashimoto, T. Takizawa, A. Fujimori, M. Kubota, K. Ono, and H. Eisaki, Phys. Rev. B **82**, 085119 (2010).

[102] M. Onoda, H. Ohta, and H. Nagasawa, Solid State Comm. **79**, 281 (1991).

[103] I. A. Nekrasov, G. Keller, D. E. Kondakov, A. V. Kozhevnikov, T. Pruschke, K. Held, D. Vollhardt, and V. I. Anisimov, Phys. Rev. B **72**, 155106 (2005).

[104] V. I. Anisimov, D. E. Kondakov, A. V. Kozhevnikov, I. A. Nekrasov, Z. V. Pchelkina, J. W. Allen, S.-K. Mo, H.-D. Kim, P. Metcalf, S. Suga, A. Sekiyama, G. Keller, I. Leonov, X. Ren, and D. Vollhardt, Phys. Rev. B **71**, 125119 (2005).

[105] A. Liebsch, Phys. Rev. Lett. **90**, 096401 (2003).

[106] M. Karolak, T. O. Wehling, F. Lechermann, and A. I. Lichtenstein, J. Phys.: Condens. Matter **23**, 085601 (2011).

[107] G. Trimarchi, I. Leonov, N. Binggeli, D. Korotin, and V. I. Anisimov, J. Phys.: Condens. Matter **20**, 135227 (2008).

[108] H. Lee, K. Foyevtsova, J. Ferber, M. Aichhorn, H. O. Jeschke, and R. Valenti, Phys. Rev. B **85**, 165103 (2012).

[109] P. Wissgott, J. Kunes, A. Toschi, and K. Held, Phys. Rev. B **85**, 205133 (2012).

[110] M. Gatti and M. Guzzo, Phys. Rev. B **87**, 155147 (2013).

[111] D. van der Marel, J. L. M. van Mechelen, and I. I. Mazin, Phys. Rev. B **84**, 205111 (2011).

[112] J. D. Pack, H. D. Monkhorst, and D. L. Freeman, Solid State Comm. **29**, 723 (1979).

[113] J. M. Tomczak, M. van Schilfgaarde, and G. Kotliar, Phys. Rev. Lett. **109**, 237010 (2012).

[114] S. Biermann and A. van Roekeghem, J. Electron Spectrosc. Relat. Phenom. **208**, 17 (2016).

[115] S. Kohiki, M. Arai, H. Yoshikawa, S. Fukushima, M. Oku, and Y. Waseda, Phys. Rev. B **62**, 7964 (2000).

[116] S. Backes, T. C. Rödel, F. Fortuna, E. Frantzeskakis, P. Le Fèvre, F. Bertran, M. Kobayashi, R. Yukawa, T. Mitsuhashi, M. Kitamura, K. Horiba, H. Kumigashira, R. Saint-Martin, A. Fouchet, B. Berini, Y. Dumont, A. J. Kim, F. Lechermann, H. O. Jeschke, M. J. Rozenberg, R. Valentí, and A. F. Santander-Syro, Phys. Rev. B **94**, 241110(R) (2016).

[117] R. Shankar, Rev. Mod. Phys. **66**, 129 (1994).

[118] T. Miyake, F. Aryasetiawan, and M. Imada, Phys. Rev. B **80**, 155134 (2009).

[119] L. Boehnke, F. Nilsson, F. Aryasetiawan, and P. Werner, Phys. Rev. B **94**, 201106(R) (2016).